ABSTRACT

THOMPSON, MARGARET OLIVIA. Rapid Small-Scale Column Test Development for Evaluating Excess Fluoride Removal from Drinking Water Using Bone-Char Sorbents. (Under the direction of Dr. Joshua Kearns).

Fluoride (F) contamination in groundwater (GW) is a globally distributed problem impacting hundreds of millions of people. Fluoride intake above the World Health Organization (WHO) guideline value of 1.5 mg/L for drinking water can lead to severe dental fluorosis and above 10 mg/L crippling skeletal fluorosis. Many communities impacted by F contaminated water are resource-scarce and rely on point-of-use (POU) systems as their main source of drinking water. For example, community wells in Guanajuato state, central Mexico, regularly exceed 2 mg/L and have been recorded up to 23.4 mg/L. Cow bone-char (BC) produced locally utilizing waste material from beef processing has shown promise as a low-cost sorbent for defluoridation of GW. Traditionally, pilot column tests have been conducted to evaluate treatment systems but are costly, time consuming, and require large amounts of water from water-scarce areas. Therefore, a bench scale method applying a rapid small-scale column test (RSSCT) approach was developed to be used in a field lab setting to quantify F removal by BC sorbents from GW specific to central Mexico. Isotherm batch and differential column batch reactor tests were conducted with different BC particle sizes to determine equilibrium (F sorption capacity) and kinetic (intraparticle diffusion coefficients) parameters following the homogeneous surface diffusion model (HSDM). Results were used to design constant (CD) and proportional (PD) diffusivity RSSCTs with crushed BC for comparison with pilot columns using full-size BC granules. CD and PD RSSCT breakthrough curves were fit with the HSDM to determine the best approach for predicting F breakthrough from actual treatment systems. Duplicate experiments were conducted using GW collected in Mexico and laboratory model GW with similar background chemistry.

This RSSCT approach will save time, labor, and experimental resources, and support the implementation of affordable POU water treatment in low resource settings.

Rapid small-scale column test development for evaluating excess fluoride removal from drinking water using bone-char sorbents.

by
Margaret Olivia Thompson

A thesis submitted to the Graduate Faculty of
North Carolina State University
In partial fulfillment of the
requirements for the degree of
Master of Science

Environmental Engineering

Raleigh, North Carolina
2020

APPROVED BY:

_____	_____
Dr. Joshua Kearns Committee Chair	Dr. Detlef Knappe
_____	
Dr. Owen Duckworth	

DEDICATION

I would like to dedicate this thesis to my parents, Trina and David Thompson for supporting me, to my uncle Daniel Thompson for encouraging my interest in STEM, and my grandfather John Raymond Thompson whose incredible life inspired me to pursue engineering.

BIOGRAPHY

Margaret Thompson graduated in May 2018 with a BS in Environmental Engineering and a minor in Soil Science from NC State. As an undergrad she conducted soil chemistry research with the Crop & Soil Science Department to determine mechanisms by which various polymers sorb to soil surfaces. Travel, fieldwork, and chemistry are among her passions. She is originally from Greensboro, NC and spent most of her childhood outside enjoying nature. She has been an active Girl Scout from the age of 6 until high school graduation when she earned her Gold Award for organizing a community stream restoration. Her involvement with the Girl Scouts sparked her interest in STEM and environmental stewardship. As an MS student, Maggie studied sorption processes for control of fluoride rich groundwater in Mexico. Maggie traveled to Guanajuato, Mexico during her MS studies working with the non-profit Caminos de Agua in the city of San Miguel de Allende.

ACKNOWLEDGMENTS

I would like to thank Mike for supporting me every day for the last four years. Sierra and Nancy Lee for being the most supportive friends and encouraging me when I needed it most. Myat for being there with me in the lab learning together. Josh for advising me and giving me the opportunity to work on such impactful research. Detlef for being a kind and helpful mentor throughout my time at NC State. Owen for encouraging me to pursue research as an undergrad. Diana and Markus for believing in me, helping me to realize my potential, and encouraging me to attend graduate school. As well as everyone I worked with at Caminos, especially Aaron, Miguel, Matthieu, Allie, and Martijn.

TABLE OF CONTENTS

LIST OF TABLES

LIST OF FIGURES

LIST OF ACRONYMS & ABBREVIATIONS

AA	Activated Alumina
AC	Activated Carbon
ACBC	Aluminum Oxide Coated Bone-char
ACWC	Aluminum Oxide Coated Wood-char
AIWC	Aluminum Oxide Impregnated Wood-char
BC	Bone-char
BV	Bed Volume
CAB	Chemically Activated Bone
CD	Constant Diffusivity
CdA	Caminos de Agua
CMBC	Chemically Modified Bone Char
DCBR	Differential Column Batch Reactor
EBCT	Empty Bed Contact Time
F	Fluoride
GAC	Granular Activated Carbon
GW	Ground Water
HSDM	Homogeneous Surface Diffusion Model
INF	Influent Fluoride Concentration
LC	Large Column
MX	Mexico
NC	North Carolina
NOM	Natural Organic Matter
PD	Proportional Diffusivity
POU	Point-of-use
PR	Polymeric Resin
RSSCT	Rapid Small-scale Column Test
SC	Small Column
TO	Treatment Objective
WaSH	Water, Sanitation, and Health
WC	Wood Char
WHO	World Health Organization

Chapter 1: Introduction

1.1. Background

Fluoride (F) contamination in groundwater (GW) is a globally distributed problem impacting hundreds of millions of people (Amini et al., 2008). Fluoride intake above the World Health Organization (WHO) guideline value of 1.5 mg/L for drinking water can lead to severe dental fluorosis and above 10 mg/L crippling skeletal fluorosis (Fawell et al., 2006). All natural waters contain some level of F and data on dental and skeletal fluorosis associated with exposure to elevated F through drinking-water has been collected for more than 30 countries (Ayoob, Gupta, & Bhat, 2008; Fawell et al., 2006). In countries where data are limited, global probability (Figure 1) based on factors such as geology and climate shows the vast reach of the problem (Amini et al., 2008). Many communities impacted by F contaminated water are resource-scarce and rely on point-of-use (POU) systems as their main source of drinking water. Although data on the extent of adverse health effects from fluoride is limited in developing countries, many communities are at elevated risk due to their reliance on these POU systems.

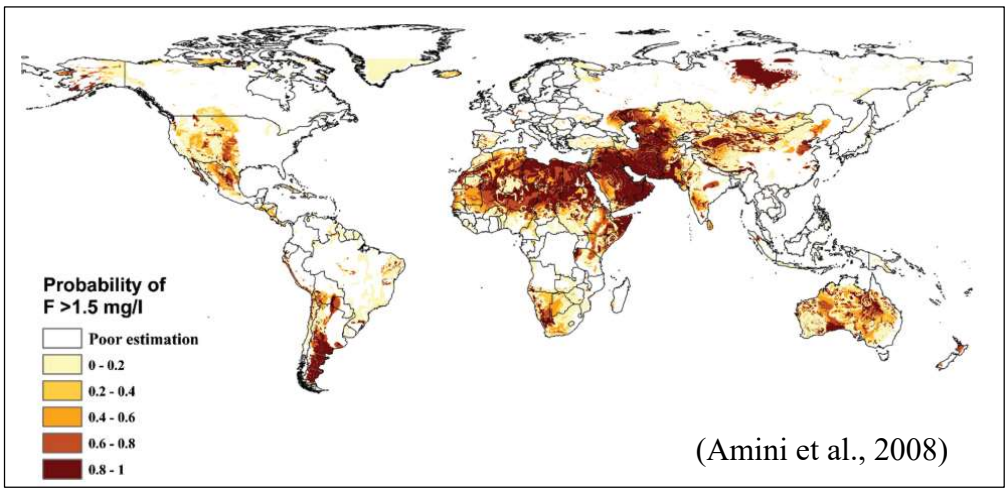

Figure 1.1. Global predicted probability of F above the WHO guideline value of 1.5 mg/L F

Largely underappreciated, fluorosis is a major environmental health problem facing many states in Mexico including Aguascalientes, Chihuahua, Coahuila, Durango, Guanajuato, San Luis Potosi and Sonora (Díaz-Barriga, Navarro-Quezada, et al., 1997). Many arid regions in Mexico rely on GW entirely for drinking water. Wells in communities across central Mexico regularly exceed 2 mg/L F and have been recorded up to 23.4 mg/L F (Caminos de Agua, 2019).

Elevated F in groundwater has been associated with various geologic conditions such as volcanic and marine sedimentary parent materials (Fawell et al., 2006). These rocks contain minerals such as fluorosilicates and fluorapatite which release F into the aquifer as they breakdown (Chatterjee, Jha, & De, 2018). Other geochemical conditions include alkaline soils with elevated pH in regions with high evapotranspiration (Amini et al., 2008). The East African Rift system has one of the most well-documented occurrences of F in groundwater of volcanic origin and has many similarities to the groundwater chemistry of central Mexico (Brunson & Sabatini, 2014; Fawell et al., 2006). Northern Guanajuato state lies atop the Alto Río Laja Aquifer within the Trans-Mexican Volcanic Belt and is known to be naturally alkaline and basic (Knappett et al., 2018). Elevated F in the aquifer is the result of this volcanic parent material and F has been increasing in community wells due to over-pumping as the region's population has increased. Within the last century, the aquifer has been depleting at a rate of 2-4 meters per year (Caminos de Agua, 2019).

1.2. Health impacts

Excess F intake can cause many health problems including dental and skeletal fluorosis. Fluorosis has been considered " the most widespread of endemic health problems associated with natural geochemistry" (Fawell et al., 2006). Many municipal drinking water facilities add F to

drinking water systems to strengthen teeth as studies have shown low levels of F, around 0.7-1 mg/L, can decrease the incidence of dental cavities (Fawell et al., 2006). The WHO (2017) has stated that F intake above 1.5 mg/L can lead to dental fluorosis, signified by staining and pitting of teeth, and above 10 mg/L crippling skeletal fluorosis, signified by osteosclerosis, calcification of connective tissue, and bone deformity. Young children are at an increased risk for these effects especially if undernourished, which is more common in rural areas of developing countries (Irigoyen-Camacho, García Pérez, Mejía González, & Huizar Alvarez, 2016). Many F exposure pathways have been identified and studied but drinking water has been determined to have the largest impact on human health (Murray, 1986). Although many places in Mexico that can afford to purchase bottled water may seem temporarily protected from the adverse health effects of drinking unsafe groundwater, bottled juice and water sampled in the city of San Luis Potosi have also been found to have elevated F (Díaz-Barriga, Leyva, et al., 1997).

1.3. Defluoridation techniques

Current defluoridation techniques include adsorption, ion exchange, precipitation, coagulation, electrochemical, and membrane removal processes (Ayoob et al., 2008; Medellin-Castillo et al., 2007). Adsorption is well suited for resource scarce areas because it does not rely on electricity (if gravity driven), does not require chemical additions, and is relatively simple to operate. The most common adsorption removal technique worldwide is the use of activated alumina (AA) due it its high selectivity for F in solution (Brunson & Sabatini, 2014; Kennedy & Arias-Paic, 2020; Medellin-Castillo et al., 2007). Limitations associated with AA include high cost (compared to other methods), complex production methods, pH dependence, and regeneration/disposal (Ayoob et al., 2008).

Bone-char (BC) produced locally utilizing waste material from beef processing has shown promise as a low-cost, effective sorbent for F removal from GW (Abaire, Zewge, & Endalew, 2009; Brunson & Sabatini, 2009; Mjengera & Mkongo, 2003). Within the last century, bone-char has been a widely available method of F removal due to its role as a decolorizing filter in the sugar industry (Ayoob et al., 2008). Ultimately, this defluoridation method declined as sugar companies moved away from bone charcoal and the product was no longer widely commercially available (Ayoob et al., 2008). In areas where bones are easily available, such as cattle ranching regions of central Mexico, bone-char can be produced on a community or household level using bones from local butcheries (Brunson & Sabatini, 2009; Fawell et al., 2006; Sorlini, Palazzini, & Collivignarelli, 2011). These raw bones are a waste product from beef processing and are traditionally used to fortify animal feed or sent to landfill. After being used for defluoridation, the spent char can either be discarded, used as a soil amendment as fertilizer, or regenerated (Fawell et al., 2006). Exposure to F through food is low and does not significantly contribute to overexposure if used as a soil amendment (Fawell et al., 2006). A life-cycle analysis of BC found it to be the least environmentally detrimental compared to other common defluoridation techniques (Yami et al., 2015). Studies comparing animal bone sources have found little defluoridation differences and concluded that widely available or culturally acceptable material may be used such as fish bone meal in coastal communities or pork bones in hog farming regions (Brunson & Sabatini, 2009, 2014; Fawell et al., 2006; Kawasaki, Ogata, Tominaga, & Yamaguchi, 2009).

1.4. Chemistry of fluoride and bone-char

Fluoride is a monovalent anion found in groundwater that can form metal complexes but is usually present in ionic form. F is the most electronegative halogen, has the same charge and relatively the same radius as hydroxide which allows for exchange on mineral surfaces (Fawell et al., 2006). BC is mainly comprised of hydroxyapatite ($Ca_{10}(PO_4)_6(OH)_2$), which is a common constituent of teeth and bones (Brunson & Sabatini, 2009). The removal efficiency of BC has been directly tied to the hydroxyapatite (HAP) content of the material (Medellin-Castillo et al., 2014). BC removal mechanisms suggested in the literature include calcium fluoride precipitation from HAP, hydroxide ion exchange to form fluorapatite, electrostatic interaction between the ion and a positively charged BC surface, and pore/surface diffusion.

Calcium fluoride (CaF_2) precipitation occurs in supersaturated F conditions where calcium and phosphate are removed from HAP following the reaction:

$$Ca_{10}(PO_4)_6(OH)_2 + 20F^- + 2H^+ \rightarrow 10CaF_2 + 6PO_4^{3-} + 2H_2O \quad (1)$$

Precipitation can only occur at very high F concentrations (20:1 F to HAP) which are not environmentally relevant (Brunson & Sabatini, 2009). Some studies have found phosphate concentration increases with F uptake (Abe et al., 2004; Kawasaki et al., 2009) but suggested F exchanges with phosphate rather than forming a precipitate. A more recent study measured the proportional increase in phosphate compared to F uptake and did not find a linear relationship disproving ion exchange with PO_4 as the only mechanism occurring between BC and F (Medellin-Castillo et al., 2014). Fluorapatite ($Ca_{10}(PO_4)_6(F)_2$) formation as the result of F ion exchanging with hydroxide has also been suggested as a potential removal mechanism following the reaction:

$$Ca_{10}(PO_4)_6(OH)_2 + 2F^- \rightarrow Ca_{10}(PO_4)_6(F)_2 + 2OH^- \quad (2)$$

This removal mechanism would result in a decrease in pH as F is taken up which has been documented depending on the influent solution pH. Suggesting this mechanism is more likely at lower pH (Fawell et al., 2006). Surface charge has been proven to impact F uptake by many studies (Chatterjee, Mukherjee, & De, 2018; Leyva-Ramos, Rivera-Utrilla, Medellin-Castillo, & Sanchez-Polo, 2010; Medellin-Castillo et al., 2014; Nigri et al., 2017). The pH_{PZC} of unmodified BC ranges from 7.6 - 10.8 depending on calcination temperature and chemical composition (Brunson & Sabatini, 2009; Chatterjee, Jha, et al., 2018; Medellin-Castillo et al., 2007; Medellin-Castillo et al., 2016). Acid modification lowers BC pH_{PZC} (4.5 - 5.5) which improves uptake over environmentally relevant pH (Medellin-Castillo et al., 2016). Other studies applying a pore diffusion model to F uptake in batch and column tests found this type of model accurately matched data and concluded pore diffusion could the rate limiting step in F uptake by BC (Chatterjee, Jha, et al., 2018; Leyva-Ramos et al., 2010; Nigri et al., 2017). Overall, the literature is not in agreement over one specific removal mechanism, though trends have been determined, a combination of multiple mechanisms is likely. For the purpose of community defluoridator design, identification of removal mechanisms are important but those impacting system operation are paramount.

1.5. Bone-char batch testing

Bacth testing is one of the first steps in understanding an adsorbent. Many studies have included batch tests to investigate F uptake by BC. These tests are used to determine sorption capacity, removal kinetics, and other characterization parameters. Important design considerations include char processing, sorbent dose, sorbate concentration, pH, temperature,

and background solution chemistry. It is also important to note equilibrium time to determine isotherm parameters accurately.

Isotherm batch tests were carried out in most studies that included BC batch testing. Isotherms provide useful sorbent-sorbate characteristic information. The two main isotherm models used in the literature are the Freundlich and Langmuir models. Both models adhere to a set of assumptions about adsorption mechanism. The Langmuir model assumes the sorbent has homogeneous surface sites for sorbate binding. This model is considered a physisorption process, although a monolayer is formed. The Langmuir equation is as follows:

$$q_e = \frac{q_m K_L C_e}{1 + K_L C_e} \quad (3)$$

Where q_e is the solid phase sorbate concentration (mg/g), q_m is the maximum solid phase concentration (mg/g), K_L is the Langmuir constant, and C_e is the liquid phase sorbate concentration (mg/L). K_L acts as the "reaction" equilibrium constant between the available surface sites and the sorbate in solution. The Freundlich model is empirically derived and assumes a chemisorption process. The Freundlich equation is as follows:

$$q_e = K_F {C_e}^{1/n} \quad (4)$$

Where q_e is the solid phase sorbate concentration (mg/g), K_F is the Freundlich capacity factor ((mg/g) $(L/mg)^{1/n}$), C_e is the liquid phase sorbate concentration (mg/L), and 1/n is the Freundlich exponent. Both models provide a term that can be related to capacity (q_m, K_F) and a measure of sorbate-sorbent affinity (K_L, 1/n).

Abe et al. (2004) was one of the first to conduct batch tests to determine temperature and pH effects on BC uptake of F. BC was compared with 11 other sorbents including activated carbons and charcoals. Batch test dosing and other experimental parameters can be found in Table 1.1 for all studies mentioned in this section. BC was found to remove the most F from

solution by a large margin over the other sorbents tested (one order of magnitude higher than the median percent F removal by all sorbents). Freundlich isotherms were plotted for all sorbents tested (see Table 1.1) with BC having the largest Freundlich capacity factor by an order of magnitude. Isotherms were also coducted at varying temperatures (10 - 40^{o}C) and a positive trend in BC sorption followed increased temperature (endothermic reaction). Batch tests were conducted at pH ranging from 4.6 to 9.2 (25^{o}C) and fluoride uptake was found to increase with decreasing pH. The researchers noted that phosphate ion in solution increased with F sorption and concluded that F was replacing phosphate on the BC surface indicating the primarily removal mechanism was ion exchange.

Medellin-Castillo et al. (2007) studied defluoridation by commercially produced cattle BC using a batch adsorber. The BC used in this study was produced in Mexico and wet sieved to a uniform diameter (d_p = 0.79 mm) before experimentation. Drinking water containing 4.02 mg/L F (pH 8.42) from San Luis Potosi, Mexico was compared with laboratory tests using F solutions at pH 7 and 10. The time to equilibrium (two consecutive F measurements of the same concentration) was determined to occur just after 1 day of reaction and tests ran for 2 to 3 days in total. BC was also compared against commercial polymeric resin (PR), activated alumina (AA), and granular activated carbon (GAC) (pH 7; 25^{o}C). BC (2.71 mg/g) outperformed AA (0.96 mg/g) and GAC (0.075 mg/g) sorption capacity but was less effective than PR (3.62 mg/g). Medellin-Castillo et al. (2007) concluded that the Freundlich isotherm better fit BC data, F sorption increased with decreasing pH (pH 3 - 12), experimental temperature (15 - 35^{o}C) did not impact uptake, and most naturally occurring ions (chloride, nitrate, nitrite, phosphate, and sulfate anions) did not significantly compete with F.

Kawasaki et al. (2009) studied BC produced by different animal sources and investigated the effects of carbonization and soprtion temperature. BC was produced from cow, pig, chicken, and fish bones at a pyrolisis temperature of either 800 or 1000ºC (BC_{800} and BC_{1000}). Fruendlich and Langmuir isotherms were calculated for all BC types and pyrolization temperatures (see Table 1.1). Kawasaki et al. (2009) found that bone type had minimal impact on sorption capacity and that BC_{800} outpreformed BC_{1000} due to exchange site degradation at elevated pyrolysis temperature. Cow BC_{800} showed increased uptake with increasing temperature (5 - 45ºC) which agreed with Abe et al. (2004). This led the reseaerchers to suggest the nature of BC adsorption of F was both physical and chemical. Kawasaki et al. (2009) measured phosphate ions in solution and concluded that F exchanged for phosphate well as participated in monolayer adsorption on the BC surface.

Brunson and Sabatini (2009) conducted batch studies comparing cow (BC_{cow}) and fish (BC_{fish}) BC produced at different pyrolyzation temperatures. The short duration (1.5 hr) BC batch tests were reacted with sodium fluoride (NaF) in distilled water at constant ionic strength. Both Freundlich and Langmuir isotherms were plotted for these sorbents (see Table 1.1) with the Freundlich model fitting data best ($R^2 = 0.99$). Brunson and Sabatini (2009) concluded that 500ºC was the optimal pyrolization temperature for BC and that BC_{fish} and BC_{cow} provided similar sorption capacity, 5.01 and 5.96 mg/g respectively (Langmuir q_{max}). Experimental pH and temperature were not included in this publication which makes direct comparison to other study findings difficult. BC_{cow} (produced at 400ºC) had the largest experimental sorption capacity for F of 5.64 ± 0.28 mg/g.

Leyva-Ramos et al. (2010) continued their work (Medellin-Castillo et al., 2007) to include kinetic modeling of the previously studied commercial cattle BC. A rotating basket

adsorber containing each particle size (d_p = 0.65, 0.79, 1.29 mm) was used in this study. Freundlich and Langmuir isotherm constants were calculated for the three particle sizes (see Table 1.1). Leyva-Ramos et al. (2010) found a slight increase in sorption capacity as particle size decreased. The researchers concluded that a larger surface area could have been created by opening previously inaccessible pores within larger particles. A diffusional model was satisfactorily applied to the data leading to the conclusion that F adsorption is controlled by pore volume diffusion rather than external mass transfer.

Sorlini et al. (2011) used batch tests to compare sorption capacity and char dose requirements for a pilot column system in Diourbel, Senegal. Cow BC used in column and batch tests was produced on-site in Senegal. Synthetic GW comprised of varying concentrations of NaF, NaCl, and K_2SO_4 in distilled water was compared with natural Senegalese GW in short duration batch tests (5 - 10 min). Sorlini et al. (2011) found that background salt (chloride and sulphate) concentration did not impact F uptake in batch tests but did see lower F removal from Senegalese GW compared to the synthetic GW solution. The researchers determined that smaller (0.2 - 0.6 mm) size char removed F more efficiently than larger granules (0.6 - 2.4 mm) over the short equilibrium time tested.

Rojas-Mayorga et al. (2013) conducted batch tests to determine kinetic, equilibrium and thermodynamic parameters of cow BC produced at an optimized pyrolysis temperature (700°C) from raw bones. Batch tests comparing pyrolysis temperature (650 - 1000°C) were plotted with both the Freundlich and Langmuir models (pH 7, 30°C). Once optimal char production was determined, BC_{700} adsorption isotherms were compared at varying pH (pH 6, 7, 8) and temperature (20, 30, 40°C). Rojas-Mayorga et al. (2013) found that F uptake increased with decreasing pH and increasing experimental temperature with greater impact from pH than from

temperature. This trend agreed with Abe et al. (2004) and Kawasaki et al.'s (2009) findings supporting F uptake by BC as an endothermic reaction. The experimental maximum fluoride uptake was found to be 7.32 mg/g for BC_{700}.

Later research by Brunson and Sabatini (2014), including batch and column studies, used charred fish bone meal in a community system in the Ethiopian Rift Valley. The fish bone-char was compared against wood char (WC), aluminum oxide coated wood char (ACWC), aluminum oxide impregnated wood char (AIWC), aluminum oxide coated bone char (ACBC), and AA as a baseline. A synthetic GW used was comprised of sodium fluoride and natural organic matter with concentrations ranging from 2.5 to 100 mg/L F. The Freundlich isotherm was plotted with this data as well as Langmuir q_{max} values (see Table 1.1). BC outperformed AA in batch tests but did not remove F as well as AIWC or ACBC. The AIWC had much larger surface area than BC, 284 ± 5.9 compared to 99.1 ± 0.8 m^2/g, which may explain the increased capacity for this material in batch tests. Untreated BC and ACBC had similar surface areas and only slightly differed in calculated isotherm parameters (see Table 1.1). Batch tests were conducted with synthetic GW while column tests were run with native GW (Meki, Ethiopia) and synthetic GW to compare breakthrough (see Section 1.7 Bone char column studies).

Medellin-Castillo et al. (2014) compared cattle BC to hydroxyapatite (HAP), the main constituent of BC (~70-90% HAP). BC was sourced and processed as before (Medellin-Castillo et al., 2007) and analytical grade HAP was used. The equilibration time for this set of batch tests was longer than the 2007 study, between 5 and 7 days, but no explanation was given for this change (see Table 1.1). Adsorption isotherms comparing BC and HAP were conducted at pH 5 and 7 (25ºC) with increased removal at the lower pH for both materials. HAP was found to have a higher sorption capacity than BC. The ratio of this difference corresponded to the percent HAP

in BC (~85%). Medellin-Castillo et al. (2014) found phosphate ion concentration did not increase proportionally to F uptake which disagreed with Abe et al. (2004) and Kawasaki et al.'s (2009) conclusion that F uptake is primarily due to phosphate ion exchange. Instead, they proposed that F removal is the result of electrostatic attraction between surface charges and is not a chemisorption process since desorption has been proven.

Medellin-Castillo et al. (2016) continued their BC research to include acid modified BC. BC was calcined (400 - 700ºC) and soaked in acid solutions (0.5 - 1.5M HNO_3) before being placed into batch adsorbers similarly used in previous studies (Medellin-Castillo et al., 2007; 2014). Equilibration time for this set of batch tests was around 7 days and tests ran for 10 days. Sorption capacity decreased with increasing calcination temperature (400 - 800ºC) as the result of decreased surface area and pore volume. Acid modification also decreased surface area in all BC tested. Acid modification, up to 1 M HNO_3, increased BC sorption capacity, despite the decrease in surface area. This was attributed to the lower pH_{PZC} for acid modified BC (3 - 4 pH units lower than unmodified char) but decreased capacity at higher concentrations (1.5 M) due to significant surface area reduction. This study found that optimum sorption (9.73 mg/g) could be achieved at a calcination temperature of 400ºC and a 1 M acid pretreatment.

Yami, Butler, and Sabatini (2016) also conducted research on chemically activated BC. Bones used in this study were treated with H_3PO_4, H_2SO_4, $ZnCl_2$, and KOH solutions, each at 20, 30, and 50 wt% before pyrolysis. Chemically activated cow bones (CAB) were compared with thermally activated cow bones (BC) by determining equilibrium capacity at 1.5 mg/L F. Yami et al. (2016) found that the CAB had higher sorption capacity than the traditional BC due to a lower pH_{PZC} (2 pH units lower than unmodified BC) and was cheaper to use due to the lower sorbent mass needed to remove the same amount of F. CAB treated with sulfuric acid (30 wt%) that was

pyrolyzed at 540ºC had the largest sorption capacity at 6.3 ± 1.1 mg/g compared to untreated BC with a capacity of 1.4 ± 0.5 mg/g. The main drawback associated with CAB implementation in developing regions is the need for reagent chemicals used in production.

Yami, Chamberlain, Butler, and Sabatini (2017) later applied their CAB method (2016) to field conditions in the town of Modjo in the Rift Valley of Ethiopia. Field produced media and laboratory produced media were statistically indistinguishable in these experiments. Yami et al. (2017) found that CAB (50 wt% KOH) outperformed BC again for removal capacity and in effect, cost. Laboratory produced bone-materials and field produced materials were both batch-tested using F solutions prepared in the laboratory. This study also included column tests run with natural well water in Ethiopia and will be discussed in the next section.

Nigri et al. (2017) also studied chemically activated cow BC. Char was purchased from a manufacturer in Maringá, Brazil where it was thermally activated between 700 and 800ºC. The BC was chemically activated by rising with 0.1 M HCl and pre-treating with solutions of $AlCl_3 \bullet 6H_2O$, $CaCl_2 \bullet 2H_2O$, $MgCl_2 \bullet 6H_2O$, $Ca(OH)_2$, or $FeCl_3 \bullet 6H_2O$. F solutions containing sodium fluoride in deionized (DI) water were compared with synthetic GW based on analyses of GW samples from northern Minas Gerais, Brazil (KCl, NaF, $MgSO_4 \bullet 7H_2O$, $NaHCO_3$, $CaCl_2 \bullet 2H_2O$, and $MgCl_2 \bullet 6H_2O$ in DI water). Nigri et al. (2017) found that F removal was fast within the first 5 hours of batch studies and slower as equilibrium was met due to pore diffusion. The Freundlich isotherm parameters for BC reacted with the F-solution had similar values compare to the synthetic GW solution with the latter having a slightly higher capacity (see Table 1.1). The pH_{PZC} was measured to be approximately 9 for BC, which agrees with Medellin-Castillo et al. (2007; 2014). Nigri et al. (2017) also developed a model based on pore diffusion to predict batch and column systems.

Chatterjee, Jha, et al. (2018) investigated BC produced from bone meal in West Bengal, India. This BC, produced from mixed animal sources (primarily chicken), was carbonized at temperatures ranging from 300 to 800ºC and sieved to 0.2, 0.3, and 0.5 mm. GW containing 3.1 mg/L F (pH 8.4) from Bankura, West Bengal, India was compared with lab solutions in batch and column tests for BC application in natural water matrix. Chatterjee, Jha, et al. (2018) measured a pH_{PZC} of 7.6; slightly lower than previously analyzed chars (Medellin-Castillo et al., 2007; 2014; Nigri et al., 2017). The Freundlich model fit data best ($R^2 = 0.99$) indicating a complex heterogeneous surface interaction between BC and F. Maximum sorption capacity was found to be 14 mg/g for BC produced at 550ºC, carbonized for 4 h with a heating rate of 60ºC/min. Chatterjee, Jha, et al. (2018) concluded that F sorption was higher for lower pH solution (pH 2 - 12), smaller particle size (0.2 - 0.5 mm), and higher experimental temperature (25 - 45ºC). Sulfate and carbonate were the only background ions to interfere with F uptake of those tested. Effective diffusivity ($6x10^{-11}$ m^2/s) and mass transfer coefficients ($9x10^{-5}$ m/s) were determined in this study and model parameters decreased in natural water systems ($3x10^{-11}$ m^2/s, $7.5x10^{-5}$ m/s). Based on the Biot number (375 - 203), Chatterjee, Jha, et al. (2018) reported that the dominant F removal mechanism was pore diffusion.

Chatterjee, Mukherjee, et al. (2018) continued their previous research to include chemically treated BC (CTBC). BC was treated with calcium oxide and aluminum sulfate after pyrolysis (300 - 800ºC). Chatterjee, Mukherjee, et al. (2018) validated their previous findings that F sorption was higher for lower pH solution and smaller particle size, but found that CTBM capacity decreased with increasing experimental temperature (25 mg/g at 30ºC; 12 mg/g at 40ºC). This suggested that due to the aluminum coating on the BC surface, F uptake by CTBM was exothermic. The pH_{PZC} of CTBM was measured to be 6.7 and compared to untreated BC at

7.6 (Chatterjee, Jha, et al., 2018). This lower pH_{PZC} allowed for a larger range of circum-neutral pH that facilitated effective removal. The CTBM in this study had a maximum sorption capacity that was an order of magnitude higher (CTBM = 150 mg/g) than untreated char (BC = 14 mg/g). This was due in part to the larger surface area of the chemically treated material (SA_{CTBM} = 110 m^2/g) compared to BC (SA_{BC} = 58 m^2/g). Phosphate was the only competing ion to significantly interfere with CTBM although other anions had a small impacted on F uptake at high concentrations.

Kennedy and Arias-Paic (2020) conducted short-duration (48 hr) batch tests to evaluate particle size impact on sorption to inform RSSCT design for BC and AA. Batch tests were conducted with BC particle sizes of 0.92, 0.21, 0.11 mm and AA particle sizes of 0.86, 0.21, 0.11 mm in raw GW. Kennedy and Arias-Paic (2020) found that the sorption capacity of each BC size fraction was not statistically different, although the mean values of smaller particle sizes were higher than the larger size ($BC_{0.11mm}$ = 2.4 ± 0.4 mg/g, $BC_{0.21mm}$ = 2.1 ± 0.3 mg/g, $BC_{0.92mm}$ = 1.9 ± 0.3 mg/g; $AA_{0.11mm}$ = 1.3 ± 0.1 mg/g, $AA_{0.21mm}$ = 1.2 ± 0.1 mg/g, $AA_{0.86mm}$ = 1.4 ± 0.2 mg/g). BC was found to have a slightly higher capacity than AA in batch tests but not in column tests (see section 1.7 Bone char column studies).

Table 1.1. Experimental conditions of batch tests and isotherm parameters from literature

Adsorbent	Raw Material	Pyrolysis Temp. (°C)	d_p (mm)	Dose (g/L)	F_o (mg/L)	pH	Exp. Temp. (°C)	Time (hr)	K_F [(mg/g) (L/mg)$^{1/n}$]	1/n	q_{max} (mg/g)	K_L (L/mg)	Reference
BC									1.06	0.39			
AC_1	Coal								0.08	0.53			
AC_2	Wood								0.04	0.68			
AC_3	Coal								0.02	0.89			
AC_4	Wood								0.02	0.99			
AC_5	Wood			10	20	7	25	3	0.02	0.70			(Abe et al., 2004)
AC_6	Petcoke								0.02	0.41			
CB									0.07	0.34			
CC_1									0.01	0.88			
CC_2									0.004	1.13			
CC_3									0.005	0.80			
CC_4									0.00003	2.58			
BC	Cow		0.79	1 or 2	1-20	7	15	48-72	2.36	0.34	6.05	0.55	(Medellin-Castillo et al., 2007)
						3	25		6.77	0.30	11.9	2.58	
						5			3.96	0.30	7.74	1.55	
						7			2.71	0.28	5.44	1.22	
						10			0.87	0.34	2.31	0.52	
						11			0.27	0.69	4.04	0.05	
						12			0.23	0.52	1.33	0.15	
						7	35		2.67	0.28	5.07	1.68	
BC	Cow	800		2			25	24	0.55	0.51	2.65	0.20	(Kawasaki et al., 2009)
	Pig								0.40	0.62	1.29	0.28	
	Chicken								0.37	0.51	2.22	0.12	
	Fish								0.36	0.42	2.25	0.21	
	Cow	1000							0.04	1.16	-0.70	-0.05	
	Pig								0.01	1.88	-0.07	-0.07	
	Chicken								0.10	0.73	1.11	0.08	
	Fish								0.00	2.32	-0.12	-0.09	
BC	Cow	400	0.29	10	5-100			1.5	0.79 [a]	0.42	5.96	0.27 [a]	(Brunson & Sabatini, 2009)
	Fish	300							0.41	0.40	2.15	0.16	
		400							0.62	0.50	5.01	0.10	
		500							0.73	0.42	4.85	0.12	
		600							0.57	0.44	3.89	0.10	
BC	Cow		0.65	0.8-2.6	3.4-22.4	7	25	48	2.84	0.33	5.70	1.16	(Leyva-Ramos et al., 2010)
			0.79						2.72	0.29	5.46	1.22	
			1.29						1.95	0.43	5.89	0.45	

Table 1.1. (continued)

BC	Cow	300-400	0.2-2.4	40	5	8.4	30	0.08-0.17 (5-10 min)					(Sorlini et al., 2011)
BC	Cow	650	1	2	10-60	7	30	24	1.92 [b]	0.31	6.88	0.23	(Rojas-Mayorga et al., 2013)
		700							2.27	0.30	7.61	0.31	
		800							1.42	0.40	7.69	0.13	
		900							0.64	0.39	3.53	0.11	
		1000							0.39	0.29	1.39	0.15	
		700				7	20		1.31	0.42	7.12	0.13	
		700				7	40		3.22	0.25	8.43	0.52	
		700				6	30		2.29	0.36	8.96	0.25	
		700				8	30		1.97	0.22	4.70	0.47	
BC	Fish	500	0.29	10	2.5-100			24	1.8	0.38	6.1		(Brunson & Sabatini, 2014)
ACBC	Fish	600							1.4	0.42	11.4		
WC	Eucalyptus								<0.1	0.82			
ACWC	Eucalyptus								0.2	0.69			
AIWC	Eucalyptus								4.6	0.61	16.8		
AA									0.4	0.48	4.1		
BC	Cow		0.79	1 or 2	1-20	5	25	120-168 (5-7 d)	3.96	0.31	7.74	1.55	(Medellin-Castillo et al., 2014)
						7			2.72	0.29	5.44	1.22	
HAP						5			5.15	0.35	10.9	1.32	
						7			2.37	0.48	11.1	0.18	
CMBC 0.5 M HNO_3 1.0 M HNO_3 1.5 M HNO_3	Cow	400, 500, 600, 700, 800	0.79	2	20	5, 7, 9		240 (10 d)					(Medellin-Castillo et al., 2016)

Table 1.1. (continued)

BC		540-500							1.3	0.3			
CAB													
30% H_2SO_4									4.6	0.7			
30%H_3PO_4									4.3	0.5			
50% $ZnCl_2$									0.4	0.5			
30% KOH									2.8	0.4			
50% KOH									3.2	0.4			
CABC													
30% H_2SO_4	Cow	540	0.29	10	0-150	7		24	4.6	0.7			(Yami et al., 2016)
30% KOH		540							2.8	0.4			
50% KOH		540							3.1	0.4			
50% $ZnCl_2$		500							1.9	0.3			
CMBC													
1000 ppm $AlCl_3$									0.9	0.6			
2000 ppm $AlCl_3$		540-500							0.9	0.5			
500 ppm $Al_2(SO_4)_3$									1.3	0.5			
1000 ppm $Al_2(SO_4)_3$									0.9	0.6			
2000 ppm $Al_2(SO_4)_3$									0.9	0.6			
CAB													
Lab-prepared	Cow		0.29	10	0-150	7		24			12.3	0.4	(Yami et al., 2017)
Field-prepared											8.8	0.4	
CABC													
HCl									2.81	0.42	6.7	0.8	
HCl + $AlCl_3$•6H2O									2.82	0.42	6.8	0.8	
HCl + $Ca(OH)_2$									1.20	0.48	4.4	0.3	
HCl + $FeCl_3$•6H2O	Cow	700-800	1.0-1.7	0.5-8.0	10	7.4	25	60	1.12	0.13	1.56	1.8	(Nigri et al., 2017)
HCl + $CaCl_2$•2H2O									2.47	0.34	5.1	1.1	
HCl + $MgCl_3$•6H2O									2.04	0.33	4.2	1.1	
Regen. w/ NaOH									1.05	0.5	4.2	0.3	
HCl (model GW)									3.2	0.38	7.0	1.0	
BC	Chicken	300-800	0.2-0.5	7	20-1000		25 35 45	24	1.1 1.3 1.6	0.36 0.33 0.31	14.0 14.4 15.3	0.016 0.013 0.015	(Chatterjee, Jha, et al., 2018)
CMBC CaO + $Al_2(SO_4)_3$	Chicken	300-800	0.2-0.5	7	20-1000		30 40 50	24	32.9 20.1 11.0	0.23 0.26 0.34	150 130 120	0.03 0.02 0.01	(Chatterjee, Mukherjee, et al., 2018)

Table 1.1. (continued)

BC	Cow	350-650	0.92 0.21 0.11	1	8.5	8.7	48	(Kennedy & Arias-Paic, 2020)
AA			0.86 0.21 0.11					

[a] Freundlich K_F reported in units of $[(mg/g)/(L/mg)^{1/n}]$ and Langmuir K_L in units of [mg/L]
[b] Freundlich K_F reported in units of [mg/g]

1.6. Differential column batch reactor tests

Few studies have used differential column batch reactors (DCBR) to quantify sorption kinetics for inorganic pollutants and none, to the authors' knowledge, have been conducted for F uptake by BC. The DCBR was first introduced by Hand, Crittenden, and Thacker (1983) to determine surface diffusion coefficients (D_s) of GAC for the removal of organic compounds. These D_s values were used to solve the Homogeneous Surface Diffusion Model (HSDM) and predict full-scale contactor performance in drinking water and wastewater treatment facilities.

Badruzzaman, Westerhoff, and Knappe (2004) were the first to apply Hand et al.'s (1983) DCBR approach to an inorganic contaminant. Arsenic uptake by granular ferric hydroxide (GFH) was studied in this paper and D_s values calculated from DCBR data were of similar magnitude to organic compounds reported in literature ($2.98x10^{-12}$ to $6.4x10^{-11}$ cm^2/s). GFH of smaller particle size exhibited faster adsorption kinetics than larger particles resulting in longer pseudo-equilibrium time for larger particles. Badruzzaman et al. (2004) found intraparticle surface diffusion to be the rate-limiting step for As uptake by GFH.

Westerhoff, Highfield, Badruzzaman, and Yoon (2005) later extended the same DCBR set-up to arsenic and GFH in rapid small-scale column tests (RSSCT) to predict full-scale contactor performance. Effective surface diffusivities for GFH were similar ($2.9x10^{-12}$ to $11.2x10^{-12}$ cm^2/s) to previous publication (2004) and followed the same relationship to particle size. D_s values were used to support the choice of the PD-RSSCT over the CD-RSSCT (see section 1.7 Bone-char Column Studies) rather than solving the HSDM for full-scale contactor prediction, although this modeling approach is mentioned as a potential use for this technique by the researchers.

1.7. Bone-char column tests

Column tests can be used to evaluate full-scale application of sorbents. Column tests are a vital link between understanding the kinetics and mechanics of adsorption (batch testing) and simulating fixed-bed contactors such as those used in many community and municipal treatment systems. Pilot columns using full-sized granular sorbent can be used to directly test the applicability of sorbents in communities. Unfortunately, pilot studies are costly, time consuming, and require large amounts for water which can be a burden on communities in water-scarce areas. Some studies included small-scale column tests to simulate pilot-scale systems to minimize resource usage.

Mjengera and Mkongo (2003) studied BC defluoridation in Tanzinia by fill-and-draw bucket-style packed column contactors. Removal systems containing BC were tested with a raw drinking water source containing 12 mg/L F and compared with an alum/lime removal technique used in a centralized treatment facility. See Table 1.2 for column test details. Inlet pH and background water chemistry (other than influent F concentration) were not included although lime was added before alum defluoridation to lower pH to optimal flocculation levels. The column-design BC contactor was found to be most efficent at removing F at high inlet concentrations compared to alum treatment. BC was determined to be appropriate for community-level application due to its local availability/production potential and operation simplicity.

Sorlini et al. (2011) conducted lab-scale columns with simulated GW and pilot columns in a community Diourbel, Senegal. More information on the BC and water used in this study can be found in the previous section. The full-scale system consisted of a bucket of media similar to Mjengera and Mkongo's (2003) design in Tanzinia. Small-columns (SC) in the lab were tested

using simulated GW and compared to the community system run with natual GW in Senegal. Sorlini et al. (2011) found that higher influent F concentration (INF) corresponded to shorter column run-time in SC tests (see Table 1.2). The two community systems (LC) were used at different rates and consistencies which corresponded to a longer lifespan of the lesser-used column (BV_{TO} = 230 vs. BV_{TO} = 410). The LC that was not used continuously also produced large dips in effluent F concentration after the raw water was in contact with BC for extended periods of time. Both LCs had the same INF (see Table 1.2).

Brunson and Sabatini (2014) were the first to apply the Rapid Small-Scale Column Test (RSSCT) method to F and BC. RSSCTs were run in a laboratory wigacth synthetic GW (deionized water and F) and compared to pilot columns set up in a community in Ethiopia treating natural GW (pH 8.2). Brunson and Sabatini (2014) applied the constant diffusivity (CD) RSSCT design approach developed by Crittenden, Berrigan, and Hand (1986). This method was originally used to evaluate GAC sorption of organic contaminants in a lab-setting. The CD-RSSCT design assumes intraparticle diffusivity does not depend on adsorbent particle size (d_p). Brunson and Sabatini (2014) found the same trend in sorption capacity in column as was found in batch tests, validating the importance of batch testing for sorbent comparison. For most materials tested (all except AA) sorbent capacity in batch tests (Langmuir q_{max}) were higher than those calculated by mass balance from columns ($q_{exhaustion}$ where $C_{effluent} = C_{INF}$. The sorbent capacity of field columns (BC_{pilot} = 3.0 mg/g) were lower than small columns (BC_{RSSCT} = 5.7 mg/g) for all sorbents tested and bed volumes to treatment objective (BV_{TO}) differed as well. The researchers suggested this was the result of differing water characteristics between lab and field experiments such as pH, competing ions, and natural organic matter (NOM).

Rojas-Mayorga et al. (2015) used micro-columns packed with BC to assess breakthrough model capability/limitations to predict adsorption patterns. Micro-columns (MC) were packed with chemically modified BC (d_p = 0.67 mm) previously produced and studied by the researchers (Rojas-Mayorga et al., 2013). Breakthrough curve shape is controlled by the dominant removal mechanism which was influenced by operating conditions (Q, INF, etc.). Breakthrough curves were steeper for higher INF making the concentration gradient higher and speeding up mass transfer. Rojas-Mayorga et al. (2015) found that a complex mathematical model (artificial neural network model) could be used to predict column breakthrough. Unfortunately, the complexity of such models might not be suitable for field systems with many variables/unknowns.

Yami et al. (2017) ran small and large columns in a community in Ethiopia to evaluate chemically activated cow-bone (CAB) and BC. The RSSCT design approach was not used in this study. The SCs were designed to compare different sorbents rather than predicting LC breakthrough, although CAB SC and LCs reached treatment objective (1.5 mg/L) at similar BVs (~ 400). Yami et al. (2017) found that CAB columns operated 4 times longer (see Table 1.2) than BC columns before reaching TO in SC and LC. This is most likely due to the increased F capacity of CAB (also found in batch tests) compared to BC (see Section 1.5. Bone char kinetic studies).

Nigri et al. (2017) conducted a column test to determine the applicability of BC treatment and breakthrough prediction by a mass transfer model. The breakthrough curve produced had an asymmetrical S-shape that slowly approached saturation (C_{out}/C_{in} = 1). This breakthrough shape is indicative of a sorption process controlled by pore diffusion and was similar to curves produced in Rojas-Mayorga et al.'s 2015 study. Nigri et al. (2017) used this curve to validate a mass transfer model based on pore diffusion that fit both batch and column data well.

Chatterjee, Jha, et al. (2018) investigated operational parameter influence on column performance with BC produced in West Bengal, India. BC of differing d_p was packed into columns a varying bed height and operated at varying flow rate and INF (see Table 1.2). The columns tested were smaller than domestic size (30 L processed per column) but could be scaled up. Chatterjee, Jha, et al. (2018) found that column performance improved (increased BV_{TO}) with increasing bed depth, decreasing flow rate, and decreasing INF. This is due to an increase in sorption sites with increasing char volume and longer contact time with slower flow rates. Removal efficiency also increased with longer bed depth and slower flow rate but decreased with lower INF. This was attributed to a weaker driving force of diffusion due to the decreased concentration gradient. Yoon-Nelson model predictions were plotted against breakthrough curves and fit data well. Column and batch tests were run with synthetic and natural GW from a community in Bankura, West Bengal, India. All tests experienced a decrease in efficiency treating natural water. The researchers attributed this to dissolved ions such as carbonate, nitrate, and sulphate competing for adsorption sites.

Chatterjee, Mukherjee, et al. (2018) repeated their column experiment (Chatterjee, Jha, et al., 2018) with chemically treated carbonized bone meal (CTBM). More information about char production and batch testing can be found in the previous section. CTBM was mixed with BC and packed into columns similarly to the previous study (see Table 1.2). Chatterjee, Mukherjee, et al. (2018) found the same relationships between operational parameters and column performance with CTBM as was found with BC in the previous study. CTBM columns were more efficient due to higher capacity compared to BC.

Kearns et al. (2018) investigated column operational strategies to improve BC defluoridation in central Mexico. Columns were run using locally produced cattle BC (d_p = 1.29

mm) and natural GW (8.5 mg/L F, pH 8.2). Columns (pilot-scale) were constructed using locally sourced materials (BV = 659 mL/column) and operated in lead-lag series and staged parallel to optimize sorbent use. Duel-column systems had a combined empty bed contact time of 76 minutes (38 minutes each) and were operated at ~18 mL/min, fed by gravity and controlled by ball valves. Kearns et al. (2018) determined a lead-lag operational strategy decreased sorbent use rate, extended replacement frequency, and decreased average effluent concentration compared to staged parallel operation for natural GW with high INF (~8.5 mg/L). Increasing BC efficiency lowers resources and cost making this method of defluoridation more feasible for developing regions.

A recent study by Kennedy and Arias-Paic (2020) applied the RSSCT approach with BC and AA to F impacted GW in Oklahoma, USA. Kennedy and Arias-Paic (2020) compared the CD-RSSCT, used by Brunson and Sabatini (2014), and proportional diffusivity (PD) RSSCT (Crittenden, Berrigan, Hand, & Lykins, 1987) to predict full-scale column performance. Similar to the CD-RSSCT, the PD-RSSCT is designed to maintain similarity between SC and LC but assumes intraparticle diffusivity depends on adsorbent particle size (d_p). AA outperformed BC in pilot columns by 200 BV to TO (BV_{AA} = 650, BV_{BC} = 450), although the AA particle size ($d_{p,AA}$ = 0.86 mm) used was slightly smaller than BC ($d_{p,BC}$ = 0.86 mm). AA had a larger surface area and pore volume than BC for all particle sizes tested, which might explain the increased F removal in AA columns. BC had a higher F removal per square meter than AA. This highlights the importance of optimizing BC surface area during char production. Neither the BC PD nor CD-RSSCT designs predicted pilot column capacity across the entire breakthrough, although the CD design did approximate curve shape well. Both SCs reached TO (1.5 mg/L) earlier than the pilot column (BV_{CD} = 200, BV_{PD} = 400, BV_{Pilot} = 450). The PD-RSSCT approximated BV to TO

better than the CD column but had a steeper breakthrough shape. EBCT was investigated using the PD column and was found not to impact sorbent use rate.

Table 1.2. Column test parameters from literature

Column Type	Adsorbent	d_p (mm)	Char Mass (g)	Bed depth (cm)	Water	F_o (mg/L)	pH	Q (mL/min)	EBCT (min)	BV (mL)	BV_{TO}	Capacity [mg/g]	Reference
LC	BC_{cow}	0.4-5	4000-5000		GW	12		100-133					(Mjengera & Mkongo, 2003)
LC	BC_{cow}	0.2-4	8000	22	GW	4.8-8.0	8.4	104 35	8		230 410	1.72 3.72	(Sorlini et al., 2011)
SC			100	13.5	GW_{model}	5 2.5		16.7		95.4	500 1000	2.88 2.90	
LC CD-RSSCT	BC_{fish}	0.64 0.30		10	GW F soln	8.6	6.0 8.2	1.2		34.5 7.9	143 100	3.0 5.7	(Brunson & Sabatini, 2014)
SC	$CMBC_{cow}$	0.67		5.4	F soln	10 25 50 100	7	3 6 3 6 3 6 3 6		4.4		3.3 4.2 7.7 8.4 13.5 11.7 14.2 18.5	(Rojas-Mayorga et al., 2015)
LC	CAB_{cow}	0.4		115	GW_1	8.9	7.8	6000[a]		47800	360		(Yami et al., 2017)
SC	CAB_{cow} BC_{cow}	0.18		10	GW_2 GW_3 GW_2 GW_3	9.3 4.3 9.3 4.3	8.3 7.8 8.3 7.8	1	7.9	7.9	400 600 117 125	4.6 2.5 1.2 1.14	
SC	$CMBC_{cow}$	1.0-1.7	12.6	28.5	F soln	9	7	1		7.1		5.96	(Nigri et al., 2017)
SC	$BC_{chicken}$	0.2-0.3		5 5 10 15 5 5 5 5	GW F soln	3.1 5 5 5 5 5 10 15	8.4 6.5	5-7.2 5 5 5 15 25 5 5	28.3 28.3 56.5 84.8 9.4 5.6 28.3 28.3	35	646 866 382 215 764 594 246 67		(Chatterjee, Jha, et al., 2018)

Table 1.2. (continued)

				20	GW	3.6	8.4	60	6.5		509		
SC	$CMBC_{chicken}$	0.2-0.3		18 20 27 20 20 20 20	F soln	5 5 5 5 5 10 15	6.5	30 30 30 40 50 30 30	11.8 4.7 17.6 9.8 7.8 13.1 13.1		340 433 462 374 297 255 128		(Chatterjee, Mukherjee, et al., 2018)
2 LCs	BC_{cow}	1.29	459 (per LC)	18	GW	8.5	8.2	18	38 (per LC)	659 (per LC)			(Kearns et al., 2018)
LC	AA BC_{cow}	0.86 0.92		17				8.4	10		650 450	19 12	(Kennedy & Arias-Paic, 2020)
CD-RSSCT	AA BC_{cow}	0.21		4.1 3.8	GW	8.5	5.9	4.8 5.1	0.6 0.5		450 200	14 6.3	
PD-RSSCT	AA BC_{cow}	0.11		14 13				2.0	1.3 1.2		510 400	13 6.9	

[a] Pilot column only operated at this flow rate for 10 hrs/day for safety reasons

1.8. Motivation

1.8.1. *Current Knowledge and Limitations*

The majority of BC defluoridation research extend only to batch testing. Most studies' primary interest is sorbent comparison or potential application of BC as an effective F sorbent. Many studies have established BC as an effective and appropriate sorbent in low-resource settings. Unfortunately, direct comparison of batch test findings between studies is difficult due to the variability in experimental design and execution. Overall, BC compared with other sorbents outperformed AA, WC, and GAC (Abe et al., 2004; Brunson & Sabatini, 2014; Kennedy & Arias-Paic, 2020; Medellin-Castillo et al., 2007) as an efficient defluoridator in batch tests but was less effective than chemically-modified BC (Brunson & Sabatini, 2014; Chatterjee, Mukherjee, et al., 2018; Medellin-Castillo et al., 2016; Nigri et al., 2017; Yami et al., 2016; Yami et al., 2017). Calcination/pyrolysis temperature of locally produced BC had a significant impact on F uptake (Brunson & Sabatini, 2009; Chatterjee, Jha, et al., 2018; Kawasaki et al., 2009; Medellin-Castillo et al., 2016; Rojas-Mayorga et al., 2013). Low temperature BC was found to retain organic matter which negatively impacts drinking water taste and quality (Fawell et al., 2006) but as BC production temperature increases, surface area and pore volume is diminished which also decreases removal capacity (Brunson & Sabatini, 2009; Chatterjee, Jha, et al., 2018; Kawasaki et al., 2009; Medellin-Castillo et al., 2016; Rojas-Mayorga et al., 2013). The most efficient cattle BC pyrolysis temperature was found to be 400-500^{o}C (Brunson & Sabatini, 2009; Chatterjee, Jha, et al., 2018; Medellin-Castillo et al., 2016).

Throughout the literature, batch tests were operated over a wide range of BC dose, initial F concentration (INF_o), and duration. Batch test dosing varied from 1 or 2 g/L (Chatterjee, Mukherjee, et al., 2018; Kawasaki et al., 2009; Kennedy & Arias-Paic, 2020; Leyva-Ramos et

al., 2010; Medellin-Castillo et al., 2007; Medellin-Castillo et al., 2014; Medellin-Castillo et al., 2016; Rojas-Mayorga et al., 2013) to 10 g/L char (Abe et al., 2004; Brunson & Sabatini, 2009, 2014; Yami et al., 2016; Yami et al., 2017) and was also tested at 40 g/L (Sorlini et al., 2011). INF_o in batch tests are important when comparing sorption capacity and isotherm parameters between studies. Most studies conducted batch tests over a wide range (0-100 mg/L) of F concentrations (Brunson & Sabatini, 2009, 2014; Leyva-Ramos et al., 2010; Medellin-Castillo et al., 2007; Medellin-Castillo et al., 2014; Medellin-Castillo et al., 2016; Yami et al., 2016; Yami et al., 2017). Few studies focused on F concentrations (5-10 mg/L) commonly found in natural GWs (Chatterjee, Mukherjee, et al., 2018; Kennedy & Arias-Paic, 2020; Nigri et al., 2017; Sorlini et al., 2011). Some studies used F concentrations above naturally occurring values (20-1000 mg/L) or did not report the concentration used in batch tests (Abe et al., 2004; Chatterjee, Jha, et al., 2018; Kawasaki et al., 2009; Rojas-Mayorga et al., 2013). This variability makes direct comparison of sorption capacity difficult between studies. Batch test duration also varied substantially across studies. The difference in equilibration time spanned minutes (Sorlini et al., 2011), hours (Abe et al., 2004; Brunson & Sabatini, 2009), days (Brunson & Sabatini, 2014; Chatterjee, Jha, et al., 2018; Chatterjee, Mukherjee, et al., 2018; Kawasaki et al., 2009; Kennedy & Arias-Paic, 2020; Leyva-Ramos et al., 2010; Medellin-Castillo et al., 2007; Nigri et al., 2017; Yami et al., 2016; Yami et al., 2017), and weeks (Medellin-Castillo et al., 2014; Medellin-Castillo et al., 2016). Equilibration time is important for capacity and isotherm parameter calculations. Estimated capacity values will be lower than actual values when batch tests are not at equilibrium. Although most sorption occurs during early times, longer batch tests (Medellin-Castillo et al., 2014; Medellin-Castillo et al., 2016) found higher capacity for BC than shorter duration tests (Abe et al., 2004; Brunson & Sabatini, 2014; Chatterjee, Jha, et al., 2018;

Chatterjee, Mukherjee, et al., 2018; Kawasaki et al., 2009; Kennedy & Arias-Paic, 2020; Leyva-Ramos et al., 2010; Medellin-Castillo et al., 2007; Nigri et al., 2017; Yami et al., 2016; Yami et al., 2017) with similar pH, particle sizes, and char production characteristics. This suggests that BC might take longer to reach equilibrium than many batch tests studies allowed.

Aside from the basic experimental framework, variables such as pH, background chemistry, and temperature have been tested. All studies that measured pH dependence of F removal found that as pH increased, F uptake decreased (Abe et al., 2004; Chatterjee, Jha, et al., 2018; Chatterjee, Mukherjee, et al., 2018; Medellin-Castillo et al., 2007; Medellin-Castillo et al., 2014; Medellin-Castillo et al., 2016; Rojas-Mayorga et al., 2013). This suggested a chemisorption mechanism due to ion exchange and an electrostatic interaction between the F ion and charged BC surface (Abe et al., 2004; Chatterjee, Jha, et al., 2018; Kawasaki et al., 2009; Medellin-Castillo et al., 2014; Medellin-Castillo et al., 2016). Two potential scenarios occur as pH lowers: (1) the BC surface exchanges phosphate/hydroxide ions for F or (2) the surface becomes positively charged by excess hydrogen ions which attracts the negatively charged F. Some studies investigated the impact of background salts but no consensus was made among findings (Chatterjee, Jha, et al., 2018; Chatterjee, Mukherjee, et al., 2018; Medellin-Castillo et al., 2007; Sorlini et al., 2011). Researchers found uptake influence from carbonate, sulfate, and phosphate at high concentrations (Chatterjee, Jha, et al., 2018; Chatterjee, Mukherjee, et al., 2018) but others found no impact at environmentally relevant concentrations (Medellin-Castillo et al., 2007; Sorlini et al., 2011). It should be noted that studies attempting to replicate natural GW characteristics saw higher F uptake in synthetic GW compared to natural waters. Experimental temperature was also investigated but findings were mixed. Most studies found a small positive correlation between temperature and F uptake (endothermic reaction) over a

temperature range (35-50°C) higher than is common in nature (Abe et al., 2004; Chatterjee, Jha, et al., 2018; Kawasaki et al., 2009; Rojas-Mayorga et al., 2013). Others found F uptake decreased with increasing temperature (exothermic reaction) (Chatterjee, Mukherjee, et al., 2018) or no impact over a lower temperature range (15-35°C) (Medellin-Castillo et al., 2007). Studies that used kinetic models to determine removal mechanisms found internal mass transfer (pore diffusion) to be the rate controlling step of adsorption (Chatterjee, Mukherjee, et al., 2018; Leyva-Ramos et al., 2010; Nigri et al., 2017).

Two main types of column tests were conducted: large-scale (full or pilot-scale) and small-scale systems. Most studies conducting column tests did so via full-scale contactor testing in communities (Brunson & Sabatini, 2014; Chatterjee, Jha, et al., 2018; Mjengera & Mkongo, 2003; Sorlini et al., 2011; Yami et al., 2017). Others ran only small-scale tests to assess column operational changes or fit models (Chatterjee, Jha, et al., 2018; Chatterjee, Mukherjee, et al., 2018; Nigri et al., 2017; Rojas-Mayorga et al., 2015). Some studies ran both small and large scale column tests but did not match small column to large column designs sufficiently and/or failed to appropriately simulate field-conditions in laboratory experiments (Brunson & Sabatini, 2014; Kennedy & Arias-Paic, 2020; Sorlini et al., 2011; Yami et al., 2017). Brunson and Sabatini (2014) and Kennedy and Arias-Paic (2020) were the only researchers to apply the RSSCT method to large-scale contactor performance prediction. This method of retaining similitude between small and large columns has shown promise as a quantitative way of assessing prediction quality. Developing a reliable RSSCT design for a field lab setting would save time, labor, and experimental resources, and support the implementation of affordable POU water treatment in low resource regions.

1.8.2. *Gaps in Research*

Many column studies comparing laboratory tests to field tests lack a clear understanding of the impacts water characteristics have on column performance. In addition, a reliable method for predicting full-scale performance (RSSCT, simple adsorption model, etc.) is also lacking from the literature.

1.9. Research Objectives

The overall objective of this research is to develop a bench-scale method for predicting F removal from groundwater by packed bed reactors containing BC. Two approaches were investigated, one following a batch test approach applied to the HSDM and one using the RSSCT approach.

The following hypotheses will be tested:

1) Experimental and modeling approaches used to predict AC performance for organic contaminant removal apply to F uptake by BC. This has previously been demonstrated by Westerhoff et al. (2005) for As removal by GFH and by Kennedy and Arias-Paic (2020) for F removal by BC.

   Research tasks:

   a. Conduct batch isotherm, kinetic, and DCBR tests to establish particle size influence on F uptake kinetics and equilibrium.
   b. Apply the HSDM using parameters found in batch tests (part 1a above) to assess model prediction of pilot columns.
   c. Conduct RSSCTs to determine the appropriate small-column design approach (CD vs. PD) for full-scale contactor performance prediction.

2) Model water will predict F capacity of BC in batch and column tests compared to natural GW specific to Mexico. Studies conducting parallel laboratory and field columns experienced increased char defluoridation capacity from simple model water (pH and salt additions) compared to natural GW in Ethiopia and India (Brunson & Sabatini, 2014; Chatterjee, Jha, et al., 2018).

   Research tasks:

   a. Conduct batch and column test in Mexico with natural GW (GW^{well}) and at North Carolina State University using synthetic GW (GW^{model}) containing similar major constituents to compare uptake capacity.
   b. Vary GW^{model} pH and silicate content to evaluate impact on F removal capacity of BC.

3) Temperature will affect F uptake in batch and column tests. Prior literature is unclear whether F uptake increases or decreases with increasing temperature over an environmentally relevant range (Abe et al., 2004; Chatterjee, Jha, et al., 2018; Chatterjee, Mukherjee, et al., 2018; Kawasaki et al., 2009; Medellin-Castillo et al., 2007; Rojas-Mayorga et al., 2013).

   Research tasks:

   a. Conduct batch and column tests at differing temperatures using GW^{model} at NC State to determine temperature influence on F removal for this system.

The hypotheses will be tested, and objectives will be met by completing the following tasks:

1) Operating pilot columns in Mexico and at NC State. (Section 2.3.4-2.3.5)
2) Conducting batch isotherm, kinetic, and DCBR tests. (Section 0-2.3.3)

3) Conducting RSSCTs in both Mexico and at NC State. (Section 2.3.4-2.3.5)
4) Applying the HSDM to DCBR and column data. (Section 2.3.6)
5) Varying GW^{model} chemical composition. (Section 2.3.7)
6) Conducting batch and column tests at differing temperatures using GW^{model} at NC State. (Section 3.4)

Motivation/desired outcomes of this research include:

- Development of a workflow for quantifying fluoride removal by bone-char sorbents from groundwater to be used in a field-lab setting.
- Present practitioners with tools necessary to determine effective defluoridation materials through the use of the RSSCT and HSDM.

Chapter 2: Bench-scale method development for predicting full-scale packed bed BC defluoridator performance

2.1. Introduction

Fluoride (F) contamination in drinking water above the World Health Organization (WHO) guideline value of 1.5 mg/L is a globally distributed problem impacting hundreds of millions of people (Amini et al., 2008; WHO, 2017). Many regions impacted are resource-scarce and rely on point-of-use (POU) systems as the main source for drinking water. For example, community wells in Guanajuato state, central Mexico, regularly exceed 2 mg/L and have been recorded up to 23.4 mg/L (Caminos de Agua, 2019). A safe, reliable defluoridation method is needed to protect public health in Mexico and many other countries around the world.

Cow bone-char (BC) produced locally utilizing waste material from beef processing has shown promise as a low-cost sorbent for F uptake from GW in communities in Ethiopia, Tanzania, Senegal, and India (Brunson & Sabatini, 2014; Chatterjee, Jha, et al., 2018; Mjengera & Mkongo, 2003; Sorlini et al., 2011). Traditionally, BC contactors have been tested at full or pilot scale to evaluate treatment system performance but are costly, time consuming, and require large amounts of water from regions facing water-scarcity (Mjengera & Mkongo, 2003; Sorlini et al., 2011). Therefore, developing a bench scale method to predict full-scale contactor performance has the potential to save time, money, and resources in developing regions.

Some studies have applied a small-column (SC) approach to BC systems to predict community-scale column performance but these approximations lacked reliable quantitative methods for scale-up (Chatterjee, Jha, et al., 2018; Nigri et al., 2017; Sorlini et al., 2011; Yami et al., 2017). Brunson and Sabatini (2014) were the first to apply the rapid small-scale column test (RSSCT) approach to a BC defluoridation system in a community in Ethiopia. The constant diffusivity (CD) RSSCT design approach developed by Crittenden et al. (1986) was applied to

this system. The CD-RSSCT method was originally used to evaluate granular activated carbon (GAC) sorption of organic contaminants and assumes intraparticle diffusivity does not depend on adsorbent particle size. Brunson and Sabatini (2014) tested their RSSCTs in a lab setting with F solution and pilot system in a community with natural GW. The RSSCT was unable to accurately predict large column (LC) performance most likely due to this difference in water chemistry. A recent study by Kennedy and Arias-Paic (2020) expanded upon the RSSCT method used by Brunson and Sabatini (2014) for F uptake by BC contactors by testing the CD-RSSCT and proportional diffusivity (PD) RSSCT (Crittenden et al., 1987). Similar to the CD-RSSCT, the PD-RSSCT is designed to maintain similarity between SC and LC but assumes intraparticle diffusivity depends on adsorbent particle size. Kennedy and Arias-Paic (2020) ran all columns (LC and SCs) with the same source water. Neither the PD nor CD-RSSCT predicted full-size contactor breakthrough across all bed volumes (BV) but curve shape was approximated with the CD and BV to treatment objective (1.5 mg/L) with the PD.

An additional method for predicting LC performance is to apply a model to simulate column break through. Studies have applied diffusion models to BC systems with some success but these models require many inputs and may not be feasible for complex, field-scale application (Chatterjee, Jha, et al., 2018; Nigri et al., 2017; Rojas-Mayorga et al., 2015). The Homogeneous Surface Diffusion Model (HSDM) is a relatively simple model that has been used and predict full-scale GAC contactor performance for the removal of organic contaminants in drinking water and wastewater treatment facilities. Westerhoff et al. (2005) suggested the application of the HSDM to an inorganic contaminant (As) sorption system could be used similarly to GAC uptake of organics. Determining primary removal mechanisms are important when using models such as the HSDM due to model assumptions therein. Systems with

intraparticle diffusion (D_s) limited by surface diffusion, such as organic chemical sorption by GAC, may be adequately modeled using the HSDM (Westerhoff et al., 2005). Systems controlled by pore diffusion would not be adequately modeled using the HSDM. Therefore, understanding diffusion controlling processes may give evidence for appropriate model application.

The objective of this research is to develop a bench-scale method for predicting F removal from groundwater by packed bed reactors containing BC. Two approaches were investigated, one following a batch test approach applied to the HSDM and one using the RSSCT approach. Both approaches aided in understanding diffusional processes between BC and F.

2.2. Methods

2.2.1. *Waters*

Groundwater (GW) for experiments conducted in the Caminos de Agua (CdA) field lab was collected from a local well in Guanajuato State (GTO) just outside the city of San Miguel de Allende (21°01'33.7"N 100°48'48.8"W). This water (GW^{well}) was collected from a deep well (50m) located on a small farm. This source has been used for many previous experiments conducted by CdA, and the groundwater chemistry is well understood. The water was also analyzed for salt ions, pH, TDS, TOC and background fluoride concentration before initial batch tests began. GW^{well} characteristics are summarized in Table 2.1. The water was spiked to 8 mg/L F with sodium fluoride (NaF) and analyzed by a portable Hach Colorimeter (DR850) following the SPADNS 2 reagent method. This concentration was chosen as the upper bound for 95% of water supplies sampled from an analysis of fluoride in wells across Guanajuato State by CdA. Water was collected in 20 L high-density polyethylene (HDPE) carboys and stored at room

temperature (25-30ºC; not climate controlled) in the CdA lab before being used for experiments. Samples taken from batch and columns tests were stored in a refrigerator and brought to room temperature just before F analysis.

A synthetic groundwater solution (GW^{model}) was prepared for experiments conducted in NC State's environmental engineering laboratory using lab-grade salts ($CaCl_2•2H_2O$, NaF, $MgCl_2•6H_2O$, KCl, Na_2SO_4, $Na_2SiO_3•9H_2O$). This solution was prepared following a representative groundwater report from Guanajuato State's Alto Río Laja Aquifer (Knappett et al., 2018). The salt solution was then analyzed by inductively coupled plasma optical emission spectroscopy (ICP-OES) analysis (Perkin Elmer ICP-OES Model 8000 Dual View, Waltham, MA) in the Environmental and Analytical Testing Services Laboratory (North Carolina State University, Raleigh, NC). GW^{model} quality parameters are listed in Table 2.1. Three batches of synthetic groundwater were prepared in NC State's environmental engineering lab. Batch 1 (GW_1^{model}) was not pH adjusted (pH 5.8), batch 2 (GW_2^{model}) was pH adjusted to 8.4, and batch 3 (GW_3^{model}) was pH adjusted to 8.4 and included 42.2 mg/L silicates to match GTO, MX concentrations reported by CdA. The groundwater solution was stored in a 100L HDPE barrel at room temperature (20-25ºC; climate controlled) until experimental use. For pH-controlled experiments, the GW^{model} was adjusted to pH 8.4 using 1 M hydrochloric acid and sodium hydroxide. Solution pH was adjusted and monitored by a Thermo Scientific™ Orion™ 3-Star pH Meter at room temperature (23ºC).

Table 2.1. Water Quality Parameters

Location	*Water*	*pH*	*TDS (mg/L)*	*TOC (mg/L)*	*Ca (mg/L)*	*F (mg/L)*	*Mg (mg/L)*	*Na (mg/L)*	*SO_4 (mg/L)*	*Silicate (mg/L)*
Guanajuato State, MX	GW^{well}	8.04	1	< 0.2	11.9	7.5	0.13	83.8	20.0	42.2
	Recipe	8.37	N/A	N/A	13.2	8.0	1.35	34.0	50.8	42.2
North Carolina, US	GW^{model}	5.8, 8.4	< 1.0	< 0.2	11.2	7.4-7.7	1.30	33.9	49.1	0, 42.1

2.2.2. *Bone-char*

Bone-char (BC) samples used in this study were produced at the CdA field laboratory following a method developed by Brunson and Sabatini (2009) and used by Kearns et al. (2018). Cow bones were collected from a local beef processing facility near San Miguel de Allende. The bones were cleaned and dried in direct sunlight for several days prior to pyrolysis in a 95 L (25 gal) steel drum retort. The drums were heated by burning wood below to reach an internal temperature of 570ºC over 2 hours (4.5 ºC/min heating rate). The vessel was then held at roughly 570ºC for 45 minutes and cooled rapidly with water to begin disassembly.

All BC was ground with ceramic mortar and pestle by hand and wet sieved with deionized (DI) water in NC State's environmental engineering lab to produce a uniform size distribution of char particles. This char processing method increases experimental reproducibility compared to mechanical crushing and dry sieving. After wet-sieving, BC was oven dried overnight (105ºC), desiccated, and stored in airtight HDPE bottles. The largest particle size used in column studies was collected between a #8 (2.36 mm) and # 30 (0.60 mm) US Standard sieve with a natural logarithmic mean diameter (d_p) of 1.29 mm. Three other size fractions used include 30x60#, 60x100#, and 100x200# corresponding to 0.40 mm, 0.20 mm, and 0.11 mm respectively. Two batches of BC were collected from the CdA production site, ground and sieved separately, and compared in column tests to establish reproducibility. The N_2 Brunauer-Emmett-Teller (BET) specific surface area and pore size distribution (by v-t method) of three BC particle

sizes (1.29 mm, 0.40 mm, 0.11 mm) were measured using an Autosorb iQ MP^3 gas adsorption analyzer (Quantachrome Instruments).

2.2.3. *Batch Kinetic and Pseudo-Equilibrium Studies*

Parallel isotherm batch tests were conducted with BC in the CdA field laboratory using GW^{well} and at NC State using GW^{model} to determine F uptake kinetic and pseudo-equilibrium parameters. Four size fractions of BC (8x30#, 30x60#, 60x100#, 100x200#) were oven dried overnight at 105ºC and cooled in a desiccator prior to weighing into 50 mL falcon tubes (VWR). Mass of char to be added was based on an estimated sorption capacity at equilibrium of 1.8 mg F/g BC (Leyva-Ramos et al., 2010; Medellin-Castillo et al., 2014). Individual tubes were dosed at 0.0, 0.9, 1.6, 2.2, 2.9, and 3.6 g BC/L solution using each BC size fraction with 20% duplicates and DI water blanks. Initial F concentration was 8 mg/L for both sets of experiments. Isotherm vials were placed on a tumbler, and F uptake by BC was quantified after 7-days, 14-days, 18-days, and 21-days of contact time. Suspensions were filtered using 0.45 μm Whatman™ nylon syringe filters and F was quantified in the filtrate using a portable Hach Colorimeter (DR850) following the SPADNS 2 reagent method. Apparent pseudo-equilibrium conditions were attained in GW^{well} after 14 days of contact time and was chosen for isotherm calculations. This experiment was replicated at NC State at ambient temperature (23ºC) and in an incubated shaker (35ºC) with pH adjusted GW^{model}.

2.2.4. *Differential Column Batch Reactor*

A differential column batch reactor (DCBR) was used to obtain kinetic parameters (intraparticle diffusion coefficients) for F uptake by different BC size fractions (d_p = 1.29mm, 0.20mm, 0.11mm) with GW^{model} (Hand et al., 1983). The DCBR is used to measure surface diffusion coefficients (D_s) more accurately than simple batch tests by minimizing film diffusion

(k_f) at a high hydraulic loading rate (Hand et al., 1983). The DCBR consist of a continuously stirred vessel containing 6.7 L of GW^{model} pumped through a column of BC (Mass = 6.7 g, Bed Volume = 10 cm^3) at a high hydraulic loading rate (Flowrate = 700 mL/min, HLR = 2.3 cm/sec). A schematic of the DCBR design can be found in the supplementary material (see Figure S.4). The mass of BC in the DCBR was chosen to remove approximately 50% of the initial F concentration (8 mg/L). The DCBR design was modeled after a study that quantified arsenate removal by ferric hydroxide (Badruzzaman et al., 2004). The DCBR apparatus consisted of an 8 L glass carboy stirred continuously by a large polytetrafluoroethylene (PTFE) coated magnetic stir bar, transparent polypropylene (PP) tubing, connected using 0.25-inch stainless steel fittings (Swagelok), a 1-inch inner diameter borosilicate glass chromatography column with Teflon end caps (DWK Life Sciences) packed with glass beads and glass wool to contain the BC and to ensure a fully developed flow field, and stainless steel pump head connected to a gear pump drive with RPM control (Cole-Parmer). Preliminary tests with DCBR columns loaded by bed volume revealed BC bed compression with smaller size fractions due to the high HLR. Therefore, subsequent tests used DCBR columns loaded on a mass basis. Samples (10 mL) were collected periodically over a two-week period. The mass of F removed for analysis was kept below 2% the initial mass in solution (Badruzzaman et al., 2004).

2.2.5. *Pilot Column Tests*

Pilot-scale columns (LC) were run in Mexico and at NC State as a baseline for bench-scale prediction. Additional information on mass transfer model parameters used in RSSCTs can be found in the supplementary material (see Table S.). Pilot columns were constructed of a 1-inch inner diameter borosilicate glass chromatography column with Teflon end caps (DWK Life Sciences) operated in up-flow. Pilot columns were designed to match full-scale contactor BC

particle size, bed depth, and EBCT by matching the Reynolds number (Re). Water throughput was reduced by a factor of 7.7 using the full-size to pilot scale-down. Both LC and SCs were connected by stainless steel fittings (Swagelok) to a high-performance liquid chromatography (HPLC) pump (Shimadzu LC-20AT) for accurate flowrate control. BC was degassed under vacuum until all visible air bubbles were removed (1-3 days) in deionized water. Adsorbent media was packed into columns atop glass beads followed by glass wool to support the char and to ensure a fully developed flow field. Char was packed by volume (bed depth) based on a bed density assumption (660 kg/m^3) across particle sizes. Column test design equations can be found in Table 2.2.

2.2.6.*Rapid Small-scale Column Tests*

RSSCTs were designed to maintain similitude to LCs following the scaling equations below. The first step to RSSCT design was particle diameter (d_p) scale-down. This follows the RSSCT design equation:

$$\frac{EBCT_{RSSCT}}{EBCT_{LC}} = \left[\frac{d_{p,RSSCT}}{d_{p,LC}}\right]^{2-X} = SF^{X-2} = \frac{t_{RSSCT}}{t_{LC}} \quad (5)$$

Where the EBCT and d_p of the RSSCT and LC are a function of the scaling factor (SF) and diffusivity factor (X). The diffusivity factor is 0 for the CD-RSSCT because this design assumes intraparticle diffusivity does not depend on adsorbent particle size. The diffusivity factor is 1 for the PD-RSSCT because this design assumes intraparticle diffusivity is proportional to adsorbent particle size. t_{pilot} and t_{RSSCT} are operation times of the pilot and RSSCT columns. The next step was to determine the Reynolds number (Re) for each column and subsequently equate the Stanton (St) and Peclet numbers (Pe):

$$\frac{v_{f,RSSCT}}{v_{f,LC}} = \frac{d_{p,LC}}{d_{p,RSSCT}} = SF \quad (6)$$

$$Re_{RSSCT} = \frac{\rho_w \, v_{f,RSSCT} \, d_{p,RSSCT}}{\varepsilon \, \mu_w} \quad (7)$$

Where $v_{f,RSSCT}$ is the hydraulic loading rate (HLR) for the RSSCT. These parameters were then used to determine the bed depth (L):

$$L_{RSSCT} = v_{f,RSSCT} \; x \; EBCT_{RSSCT} \quad (8)$$

It is important to note for the PD-RRSCT design, in order to match the Re_{LC} to Re_{SC} the bed depth must remain the same ($L_{RSSCT} = L_{LC}$). A method for achieving similitude when $L_{RSSCT} = L_{LC}$ is not feasible in a lab (e.g. $L_{RSSCT} > 1$ m) is called the minimum Reynolds number (Re_{min}) approach but was unnecessary in this study.

RSSCTs were constructed of translucent 3/16" (0.48cm) and 3/8" (0.95cm) inner diameter PP tubing for PD and CD-RSSCT designs, respectively. All other materials used were the same for SC as LCs. Column test design parameters can be found in Table 2.2.

Table 2.2. Column Operational Parameters

Parameter	*Pilot Column*	*CD-RSSCT*	*PD-RSSCT*
Mesh Size	8x30#	60x100#	100x200#
Particle Diameter (mm)	1.29	0.20	0.11
EBCT (min)	30.0	0.70	2.53
Column Diameter (cm)	2.54	0.95	0.48
Bed Depth (cm)	18	2.74	18
HLR (m/hr)	0.36	2.36	4.28
BC Mass (g)	60.2	1.29	2.12

Columns operated in Mexico and at NC State followed the same design parameters.

2.2.7. *Modeling*

The Homogeneous Surface Diffusion Model (HSDM) was used to apply mass transfer parameters to describe F uptake by BC in DCBR and column systems. The software Fixed-bed Adsorption Simulation Tool (FAST) was used to produce model fits applying the HSDM (Schimmelpfennig & Sperlich, 2011) to DCBR data and column breakthrough. Inputs to the

model include column design parameters such as EBCT, adsorbent mass, particle density (ρ_p), d_p, influent F concentration (INF), and column operation time. Equilibrium and kinetic parameters are used to control breakthrough curve shape. Two mass transfer parameters are required, the film diffusion coefficient (k_L) and surface diffusion coefficient (D_S). Isotherm parameter from either the Langmuir or Freundlich models are also required (K_F and 1/n or q_{max} and K_L).

2.3. Results

2.3.1. *Bone-char Characterization*

Three BC particle sizes were analyzed and were found to have a similar surface area (Table 2.3). This surface area (SA) is at the upper end of values reported in literature (82-134 m^2/g) (Brunson & Sabatini, 2009; Cheung, Choy, Porter, & McKay, 2005; Kearns et al., 2018; Kennedy & Arias-Paic, 2020; Medellin-Castillo et al., 2007; Medellin-Castillo et al., 2016). The largest size fraction analyzed (d_p = 1.29 mm) had a greater proportion of micropore area (10%) than the smaller sizes (0.2%, 3%). This may explain the difference in sorption kinetics between 8x30# size fraction and smaller sizes (see Section 2.3.3).

Table 2.3. Surface area and pore size distribution of BC

Size Fraction	*d_p (mm)*	*BET*	*V-t method*		*Reference*
		Surface Area (m^2/g)	*External Surface Area[a] (m^2/g)*	*Micropore Area[b] (m^2/g)*	
8x30#	1.29	168	147	17.4	This study
30x60#	0.40	131	130	0.3	
100x200#	0.11	150	146	4.5	
8x30#	1.29	114			(Kearns et al., 2018)
12x40#	0.92	82			(Kennedy & Arias-Paic, 2020)
60x80#	0.21	87			
100x200#	0.11	87			

[a] External surface area: pore size > 0.2 nm
[b] Micropore surface area: pore size < 0.2 nm

2.3.2.*Batch Tests*

Batch tests were conducted with GW^{model} in North Carolina and with GW^{well} in Mexico to establish preliminary equilibrium time and capacity for each bone char size fraction. Pseudo-equilibrium was achieved after 14-days for both waters and isotherm parameters were calculated with 14-day data. The majority of F uptake took place during early times and slowly reached a plateau approaching the 14-day pseudo-equilibrium time (See Figure S.2 in Supplementary Information). The Freundlich isotherm model fit the data best (R^2_{NC} = 0.99, R^2_{MX} = 0.94) although the Langmuir model also fit data well (R^2_{NC} = 0.98, R^2_{MX} = 0.92). The Freundlich isotherm parameters and corresponding 95% confidence intervals (CI) were calculated using an excel data sheet provided by the USDA utilizing a non-linear solver method (Bolster, 2010). The 95% CI calculated from the NC data were smaller than the MX data, with most fitted parameters falling within the other CIs (see Figure 2.2). A comparison of sorption capacity at equilibrium shows that particle size does not increase sorption capacity. This disagrees with literature that found a decrease in particle size resulted in a proportional increase in sorption capacity in batch tests (Chatterjee, Jha, et al., 2018; Sorlini et al., 2011) and agrees with Kennedy and Arias-Paic's (2020) recent finding that sorption capacity is independent of particle size over a similar range.

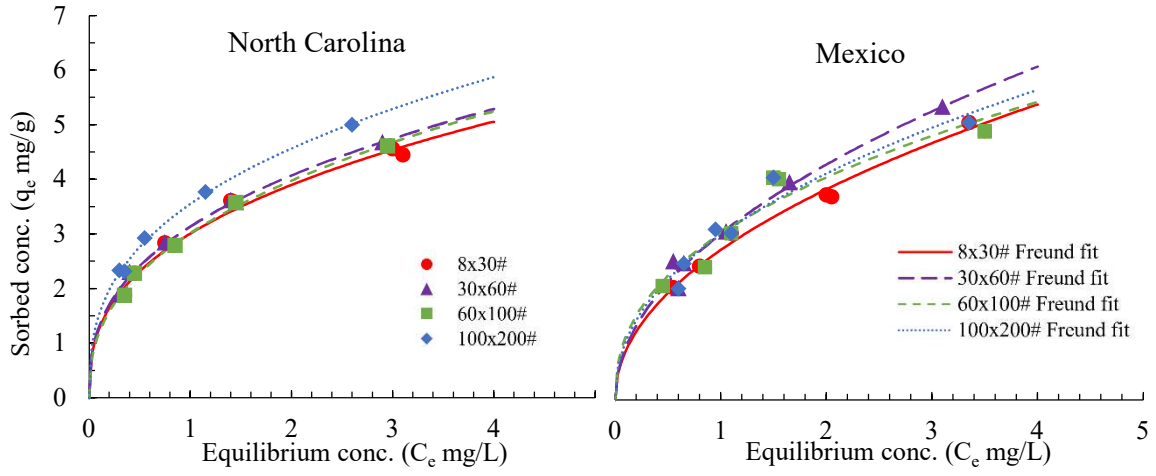

Figure 2.1. Plots of sorbed concentration vs. dissolved concentration fitted with a Freundlich isotherm model

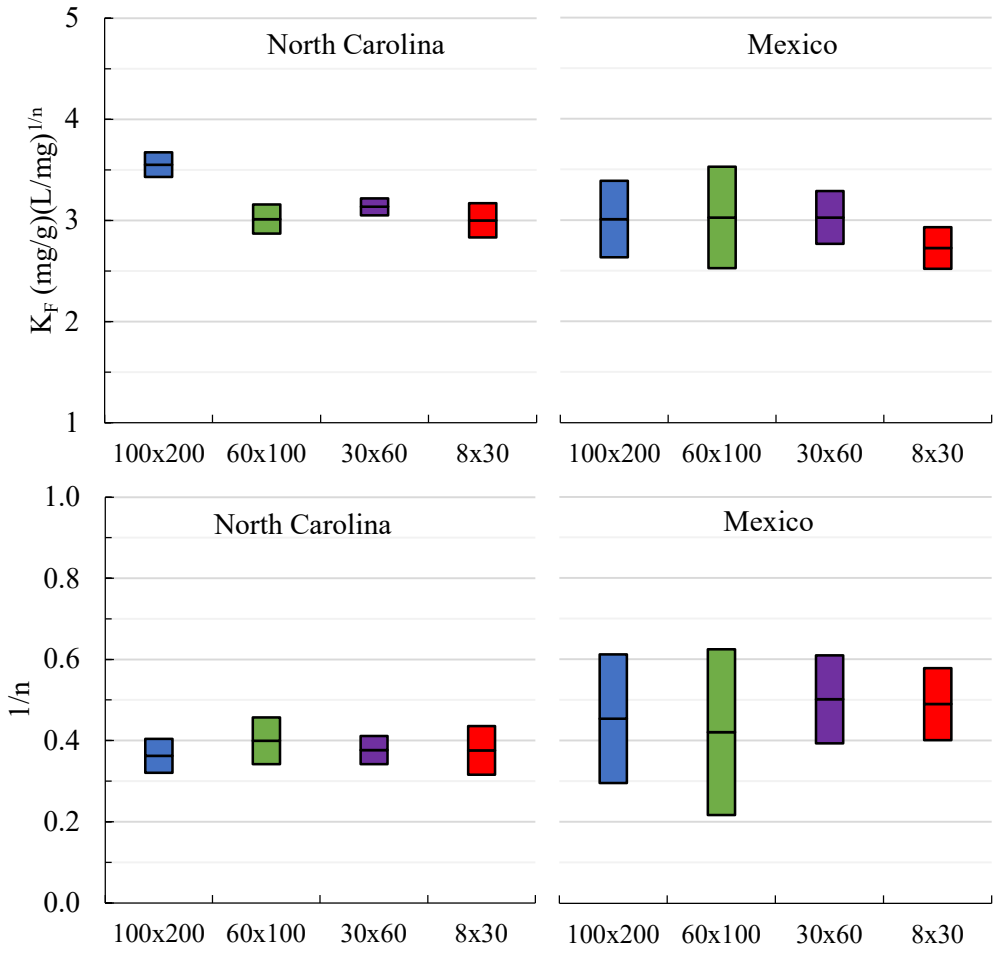

Figure 2.2. 95% confidence intervals of Freundlich parameters from USDA spreadsheet

2.3.3. *Differential Column Batch Reactor*

The DCBR produced similar curves for each particle size differing mainly in F removal kinetics and lesser by equilibrium concentration. This supports what was found in batch tests equilibrated for 14-days and is supported by Fick's second law of diffusion which states that adsorption rates are inversely proportional to the square of the particle radius. All three BC particle sizes tested in DCBRs came to similar pseudo equilibrium after 14-days but the shape of the curve produced by the largest particle size (d_p = 1.29 mm) was less steep than the smaller particle sizes (d_p = 0.49, 0.11 mm). Badruzzaman et al. (2004) found a similar kinetic relationship with GFH uptake of As but found that the pseudo equilibrium As concentration for

the larger particle size was distinctly higher than for the smaller size. The order of pseudo equilibrium F concentration for the three BC particle sizes does not follow a size relationship ($q_{equilibrium}$ = 0.49 < 1.29 < 0.11 mm). This suggests that particle size may impact uptake kinetics in community system which influences breakthrough curve shape and in effect, BC use rate. Assuming this system follows the HSDM, curve shape in DCBR studies is controlled by diffusion. The HSDM was applied to DCBR data and D_s values were estimated (see Section 2.3.6).

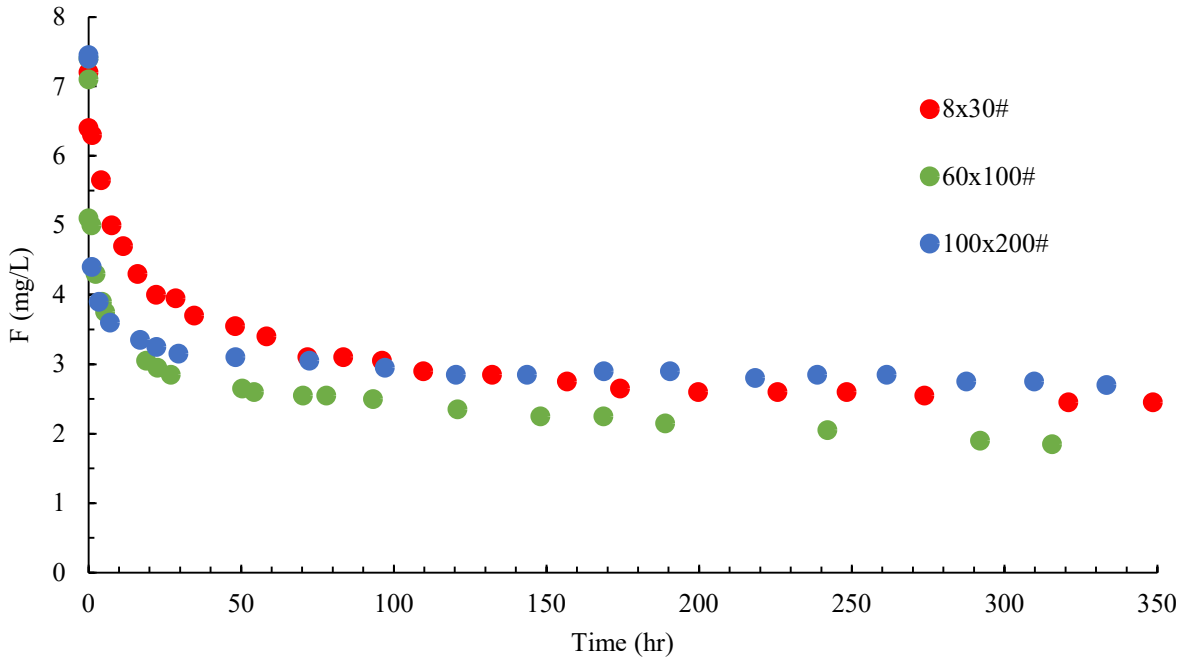

Figure 2.3. DCBR packed by mass, equilibrated for 14 days (GW^{model})

2.3.4. *Laboratory Column Tests: North Carolina, United States*

2.3.4.1. *Pilot Column*

The North Carolina pilot column breakthrough curve (run with GW^{model}) and HSDM best-fit curves are shown in Figure 2.4 with throughput in BVs (2 BV/hr). The HSDM best-fit curves were plotted alongside column data to evaluate column parameters governing curve shape. Sudden breakthrough occurred after approximately 360 BV (180 hr) and treatment

objective, 1.5 mg/L, was met after 442 BV (221 hr). The equilibrium sorption capacity of this column was calculated to be 4.0 mg/g using Freundlich parameters from the HSDM best-fit. This capacity is slightly higher than that calculated from batch test data of the same particle size (3.5 mg/g). Brunson and Sabatini (2014) found a smaller BC capacity value of 3.0 mg/g in their community LC test using BC produced from fish. This lower capacity is most likely due to the difference in water chemistry between GW^{model} and the raw GW used in Brunson and Sabatini's (2014) community system. Kennedy and Arias-Paic (2020) found a much higher BC capacity in BC pilot tests (12 mg/g). This is most likely due to the lower pH (5.9) influent water used by Kennedy and Arias-Paic (2020). Table 2.4 shows a complete comparison of column performance.

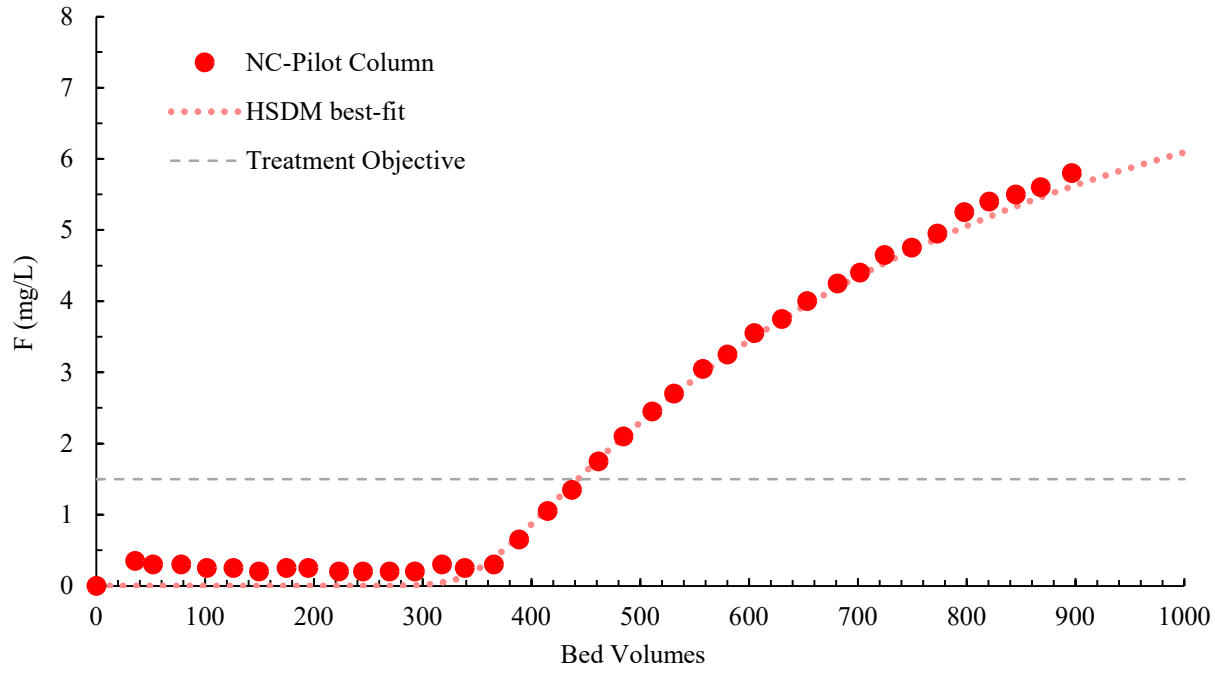

Figure 2.4. NC pilot column run with GW^{model} (pH 8.5, 25°C)

2.3.4.2. *CD-RSSCT*

The CD-RSSCT breakthrough curve can be seen in Figure 2.5 alongside the corresponding pilot column breakthrough curve and HSDM best-fits for each column. The CD-

RSSCT underpredicted bed volumes to treatment objective (BV_{TO}) for the pilot column by 75 BV but matched pilot data around 50% capacity at 4 mg/L F (658 BV). Brunson and Sabatini (2014) also found BC CD-RSSCTs underpredicted LC BV_{TO} by 43 BV but a direct comparison between SC and LCs are difficult to make due to differences in water chemistry in that study. Equilibrium sorption capacity for the CD column was calculated to be 4.8 mg/g using Freundlich parameters from the HSDM best-fit. This capacity is higher than that calculated from batch test data of the same particle size, 3.5 mg/g, and pilot column equilibrium capacity. Brunson and Sabatini (2014) found a similar BC capacity relationship between CD and pilot values, 5.7 mg/g and 3.0 mg/g respectively, but with a larger difference. Kennedy and Arias-Paic (2020) also found higher BC capacity in CD tests (6.3 mg/g) than was found here. Conversely, Kennedy and Arias-Paic's (2020) pilot columns had higher capacity than CD (almost double). The CD-RSSCT in this study was unable to predict curve shape but may be useful for approximating 50% breakthrough and providing a conservative estimate of pilot column BV_{TO}.

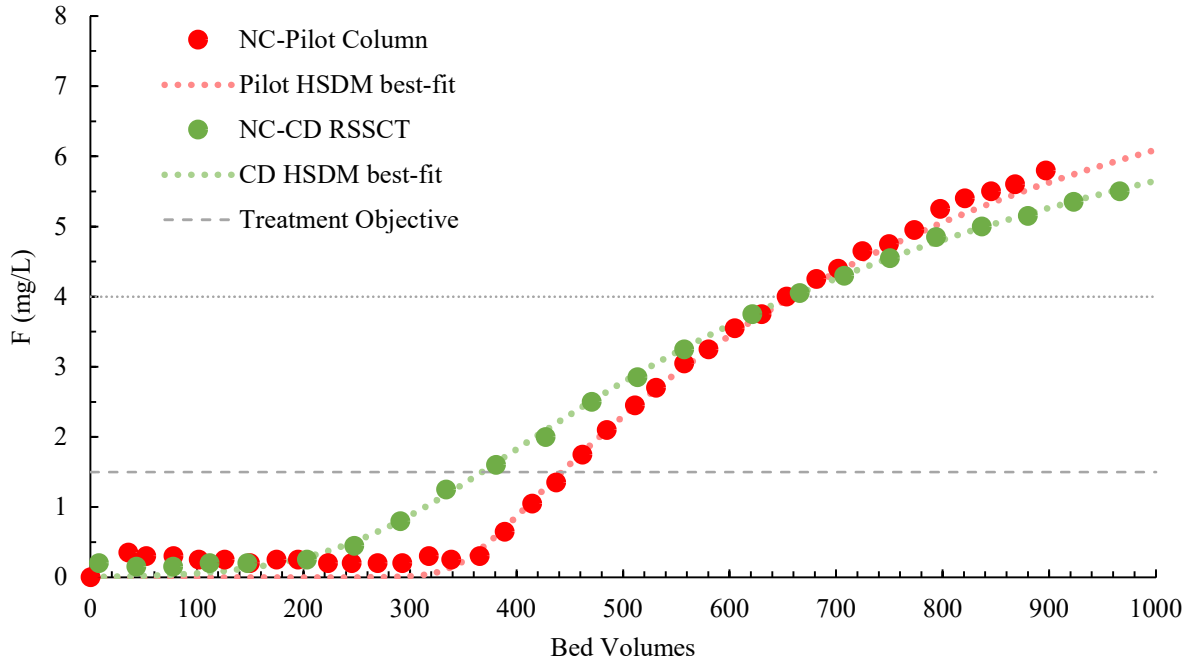

Figure 2.5. CD-RSSCT plotted with pilot column and HSDM best-fit (pH 8.4, 25ºC)

2.3.4.3. *PD-RSSCT*

The PD-RSSCT breakthrough curve can be seen in Figure 2.6 alongside the NC pilot column breakthrough curve and HSDM best-fits. The PD-RSSCT predicted BV_{TO} accurately (440) but did not match pilot column data at later BVs (after ~ 500 BV). Equilibrium sorption capacity for the PD column was calculated to be 4.4 mg/g. Similarly to the CD column, this capacity is slightly higher than that calculated from batch test data of the same particle size (4.1 mg/g) and that calculated for the pilot column (4.0 mg/g). Kennedy and Arias-Paic (2020) found similar breakthrough results from PD and pilot columns with treatment objective met after 400 and 450 BV, respectively. BC equilibrium capacity calculated from BC PD-RSSCTs in Kennedy and Arias-Paic's (2020) study were also higher than what was found in this study (6.9 mg/g) most likely due to the lower influent pH. The PD-RSSCT treating GW^{model} predicted curve shape better than the CD at early times and may provide a more accurate estimate of pilot column BV_{TO}.

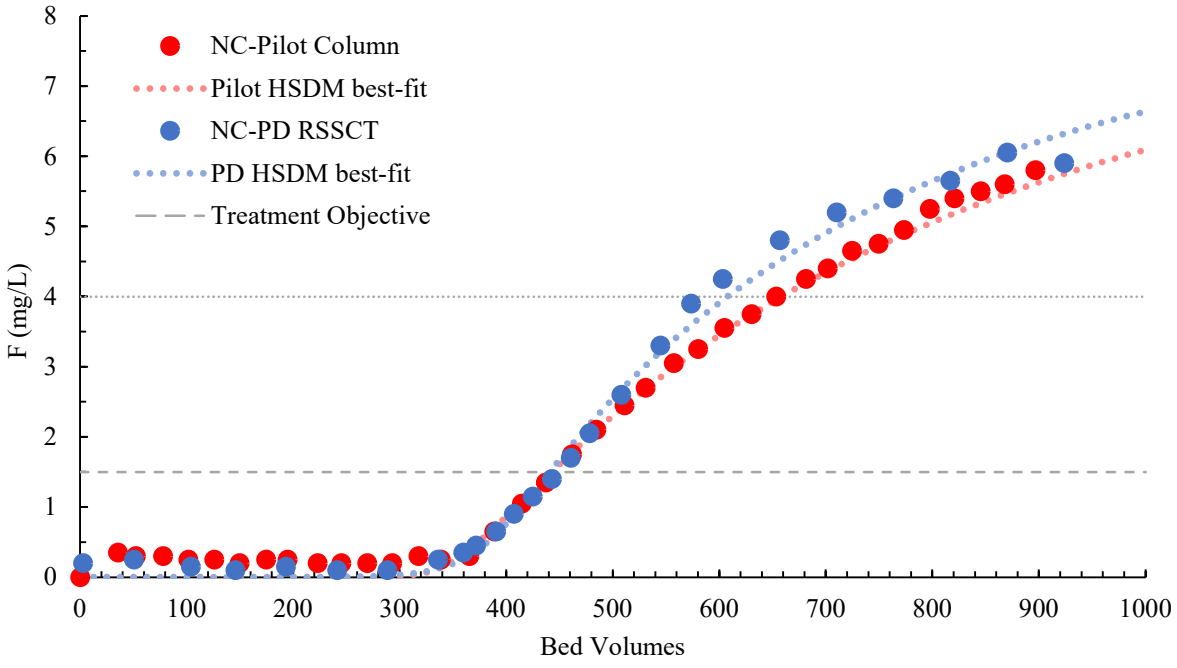

Figure 2.6. PD-RSSCT plotted with pilot column and HSDM best-fit (pH 8.4, 25°C)

2.3.5. *Field-laboratory Column Tests: Guanajuato, Mexico*

2.3.5.1. *Pilot Column*

The Guanajuato pilot column breakthrough curve (run with GW^{well}) is shown in Figure 2.7. The HSDM fit well at early BV but was unable to accurately match data beyond ~600 BV. The pilot column run in Mexico (MX-Pilot) had a steeper breakthrough shape than was found in NC with GW^{model} (NC-Pilot). Treatment objective was achieved after 310 BV for the MX-Pilot, 132 BV earlier than the NC-Pilot. This is most likely due to differences in water chemistry between GW^{model} and GW^{well}. Other studies comparing model GW with natural GW also found a decrease in column performance treating natural GW (Brunson & Sabatini, 2014; Chatterjee, Jha, et al., 2018; Sorlini et al., 2011). Equilibrium sorption capacity for the MX-Pilot column was calculated to be 2.7 mg/g. This capacity is smaller than that calculated by batch test data of the same particle size and water (3.3 mg/L) and the capacity of the NC-Pilot (4.0 mg/L).

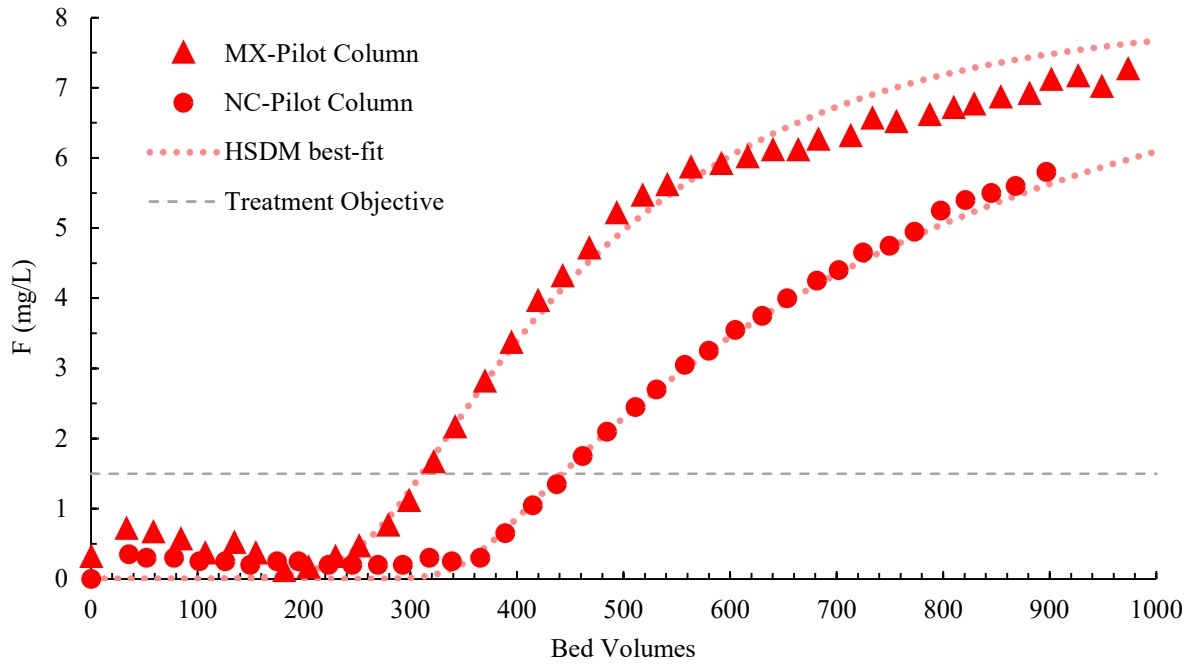

Figure 2.7. MX pilot column run with GW^{well} plotted with NC-Pilot and HSDM best-fits

2.3.5.2. *CD-RSSCT*

The CD-RSSCT (MX-CD) breakthrough curve can be seen in Figure 2.8 alongside the corresponding pilot column breakthrough curve and HSDM best-fits for each column. The MX-CD underpredicted BV_{TO} for the MX-Pilot breakthrough by 104 BV and had a gradual slope with breakthrough beginning almost immediately. Similar to the NC columns, the MX-CD also predicted 50% capacity for the MX-Pilot (430BV). Equilibrium sorption capacity for the MX-CD column was calculated to be 3.4 mg/g using Freundlich parameters from the HSDM best-fit. This capacity is slightly smaller than that calculated from batch test data of the same particle size, 3.6 mg/g, but larger than MX-Pilot column equilibrium capacity (2.7 mg/g). The CD-RSSCT, operated with natural GW, approximated 50% breakthrough, and provided a conservative estimate of pilot column BV_{TO} although capacity was diminished (compared to GW^{model} runs).

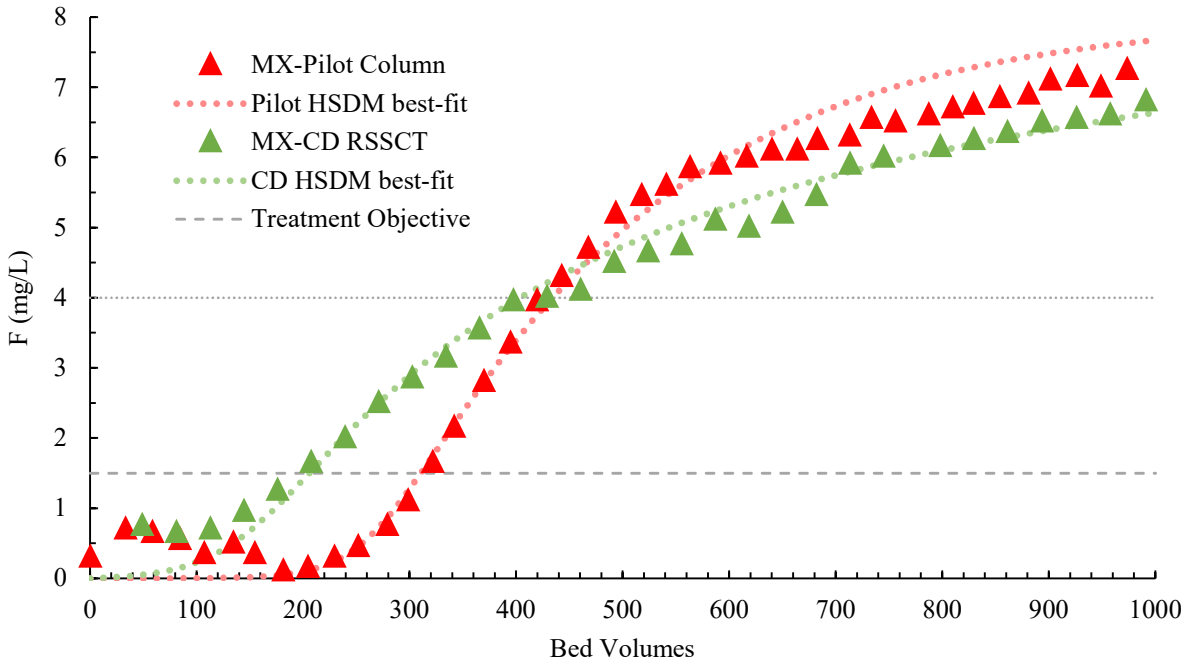

Figure 2.8. Field lab CD-RSSCT plotted with field lab pilot column

2.3.5.3. *PD-RSSCT*

The PD-RSSCT (MX-PD) breakthrough curve can be seen in Figure 2.9 alongside the MX-Pilot breakthrough curve and HSDM best-fits for each column. The MX-PD did not predict BV_{TO} as the NC-PD column did. The HSDM fits for later breakthrough did not match column data well for the MX-Pilot or MX-PD due to a plateau in breakthrough occurring after about 600 BV. The PD predicted the steep shape of the pilot curve but over-predicted BV_{TO} by 128 BV. Equilibrium sorption capacity for the MX-PD column was calculated to be 4.0 mg/g. This capacity is slightly higher than that calculated from batch test data of the same particle size (3.6 mg/g) and that calculated for the pilot column (2.7 mg/g). The MX-PD treating GW^{well} predicted curve shape better than the MX-CD but was unable to accurately predict the BV_{TO} for the MX-Pilot column.

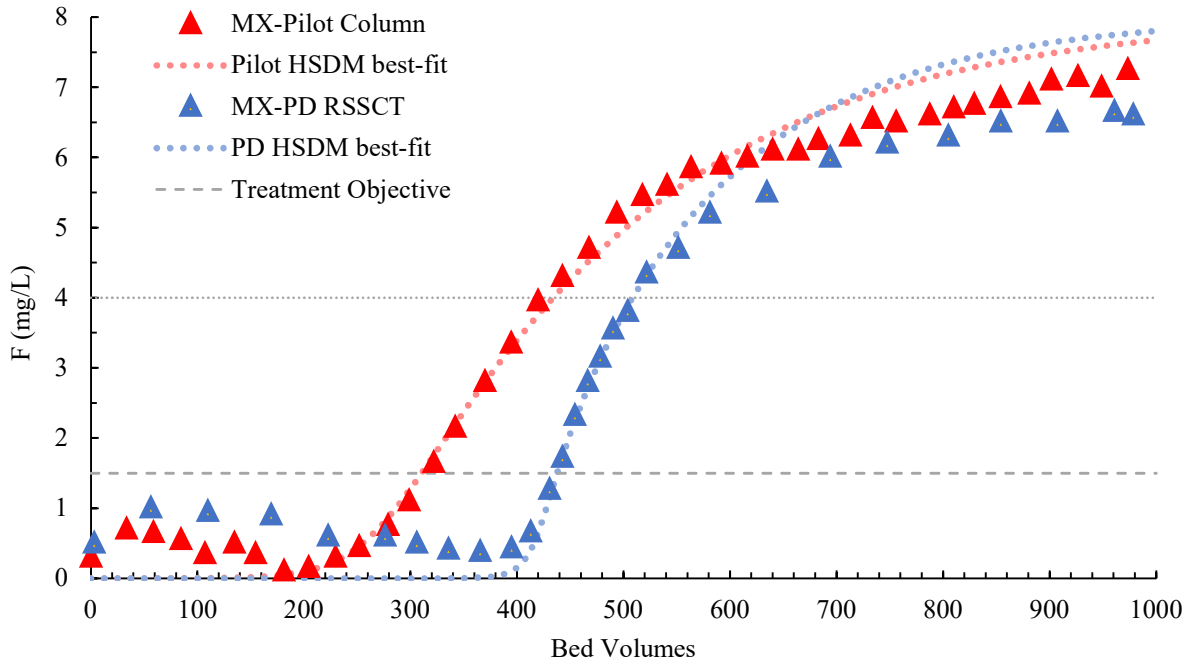

Figure 2.9. Field lab PD-RSSCT plotted with field lab pilot column

Table 2.4. Column performance summary

Location	*Water*	*Column*	BV_{TO} [a]	$BV_{50\%}$ [b]	$BV_{75\%}$ [c]	$q_{capacity}$ *(mg/g)*	*Reference*
NC, USA	GW^{model}	Pilot Column	**442**	**658**	978	4.0	This Study
		CD-RSSCT	367	**658**	1106	4.8	
		PD-RSSCT	**440**	607	860	4.4	
GTO, MX	GW^{well}	Pilot Column	310	**433**	616[d]	2.7	
		CD-RSSCT	206	**430**	769	3.4	
		PD-RSSCT	438	508	694[d]	4.0	
MER, ET	Raw GW	Pilot Column	143			3.0	(Brunson & Sabatini, 2014)
	F Soln	CD-RSSCT	100			5.7	
OK, USA	Raw GW	Pilot Column	450			12	(Kennedy & Arias-Paic, 2020)
		CD-RSSCT	200			6.3	
		PD-RSSCT	400			6.9	

[a] BV_{TO} = treatment objective; 1.5 mg/L
[b] $BV_{50\%}$ = 50% capacity; 4 mg/L
[c] $BV_{75\%}$ = 75% capacity; 6 mg/L
[d] HSDM fits for later breakthrough did not match column data well for the LC and PD in MX. These values were interpolated from data rather than HSDM best-fit.

2.3.6. *Homogeneous Surface Diffusion Model*

The HSDM was used to evaluate the relationship between various kinetic and equilibrium parameters on DCBR and column breakthrough curves. The HSDM was applied to DCBR data using the FAST to determine D_s (see Figure 2.10). The two DCBR column packing methods (by volume vs. mass) resulted in different equilibrium F concentrations and as a result, D_s (See Figure S.6 in supplement). D_s calculated from early and late equilibrium times differed over a range of half an order of magnitude for each size fraction as well. DCBR kinetic and equilibrium parameters were used to predict full-scale contactor performance but failed to accurately approximate curve shape or BV_{TO} (see Figure S.7). A sensitivity analysis was conducted on all equilibrium and kinetic inputs to the HSDM around column best-fit curves (see Figure S.8). Isotherm parameters (1/n and K_F) were varied over the 95% CI calculated from batch test data (see Figure 2.2). Mass transfer parameters (D_s and k_L) were varied over a half order of magnitude and full order of magnitude around the column best-fit corresponding to differences in values found via DCBR and best-fit HSDM plots. From this sensitivity analysis, prediction of column

performance from batch test and DCBR data was found to be difficult due to the sensitivity to changes in D_s and 1/n. These parameters control breakthrough curvature and are difficult to measure accurately in a laboratory setting for column prediction.

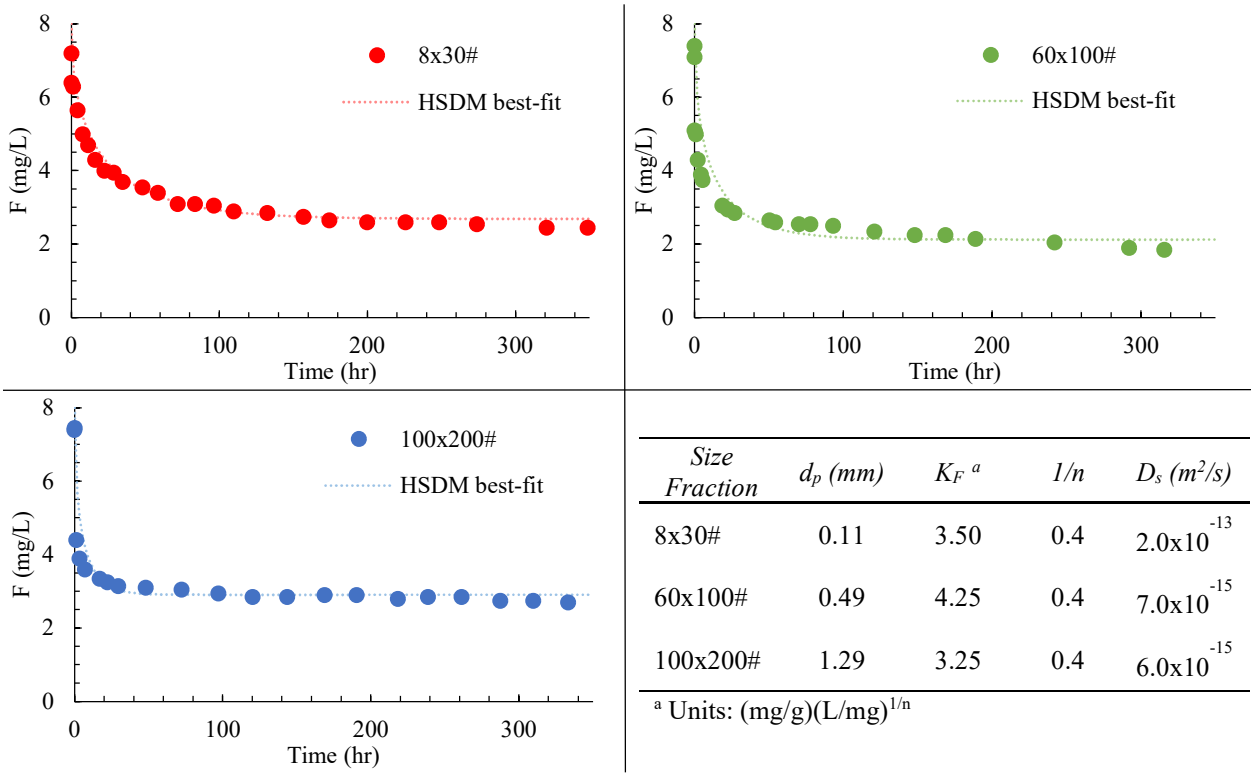

Size Fraction	d_p *(mm)*	K_F [a]	*1/n*	D_s *(m^2/s)*
8x30#	0.11	3.50	0.4	2.0×10^{-13}
60x100#	0.49	4.25	0.4	7.0×10^{-15}
100x200#	1.29	3.25	0.4	6.0×10^{-15}

[a] Units: $(mg/g)(L/mg)^{1/n}$

Figure 2.10. HSDM fits using FAST software for mass-packed DCBR (GW^{model}) fit to late equilibrium time.

2.3.7. *Experimental Factors*

A few experimental factors were investigated to determine impact on column performance. These factors included BC production batch, GW^{model} background chemistry, and experimental temperature.

Two batches of BC were compared via CD-RSSCT with GW^{well} in GTO, MX. BC batch 1 and 2 produced similar breakthrough curves differing only in breakthrough onset (see Figure S.10). BV_{TO} for each CD column differed by 50 BV while curve shape remained the same.

GW^{model} background chemistry was investigated by varying pH and silicate content. pH was not adjusted in an initial NC-Pilot run (pH 5.8) and was compared with a duplicate run with

pH adjusted to 8.4 (see Figure S.11). The pH difference between the two column runs did not impact curve shape and both columns reached TO after 440 BV. A preliminary CD-RSSCT was run with GW^{model} containing no silicates. To investigate the impact of silicate content on column performance, a second batch of GW^{model} was prepared with a silicate content similar to that recorded in GW^{well}. A CD-RSSCT was conducted with this silicate-containing GW^{model} and produced an identical breakthrough curve to the column run without silicates (see Figure S.12). The final experimental factor tested was temperature. Experimental temperature was varied to determine the impacts on column and batch test defluoridation. All three types of columns and a 14-day batch kinetic test were operated at 35ºC and compared with tests run at ambient laboratory temperature (20ºC) using GW^{model} at pH 8.4. Results from this set of experiments was mixed (see Figure S.13). The CD-RSSCT operated at 35ºC broke through early indicating an increase in experimental temperature decreases column performance. The 35ºC PD-RSSCT produced conflicting results indicating an increase in column performance at the elevated temperature. This PD-RSSCT was repeated to establish reproducibility and had the same result. A pilot column was run at 35ºC to determine the impact on a system containing full-size media. This pilot produced a similar breakthrough curve to the column conducted at 20ºC indicating that the change in temperature had no impact on column performance. A kinetic batch test sampled at intervals over a two-week period in an incubated shaker at 35ºC and 20ºC showed no influence on F uptake. Therefore, the impact of temperature is still unknown based on these findings.

2.4. Conclusions

The RSSCT approach developed by Crittenden et al. (1986; 1987) was applied to packed bed contactor systems containing BC for the treatment of elevated F in synthetic and natural GW

specific to central Mexico. Full-scale column performance treating synthetic GW was adequately predicted (BV_{TO}) using the PD-RSSCT. The CD-RSSCT provided a conservative approximation of column performance (BV_{TO}) and predicted 50% capacity when treating both synthetic and natural water. LC and SC tests showed that natural GW decreases column performance compared to synthetic GW, although some column relationships spanned water types. This highlights the importance of operating SCs with the same water as will be treated with full-scale contactors to improve prediction performance. The application of the HSDM provided a useful tool for assessing kinetic and equilibrium parameters impacting curve shape but was unable to predict column performance using batch and DCBR test data as inputs. The sensitivity analysis conducted on the HSDM best-fit curves indicated D_s had the largest impact on curve shape and breakthrough. Beyond this research, the RSSCT method could be applied to other BC materials and GW matrix to further validate the LC prediction capability.

Chapter 3: Supplementary Information

3.1. Background

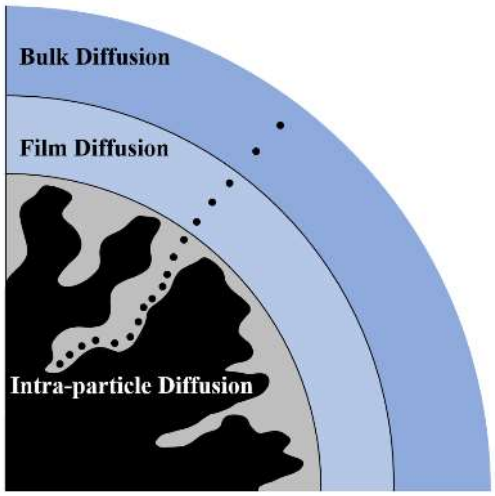

Figure S.1. Mass transfer diagram.
Depiction of sorbate (F^-) transport from bulk solution into BC pore (adapted from Badruzzaman et al. (2004)).

3.2. Batch tests

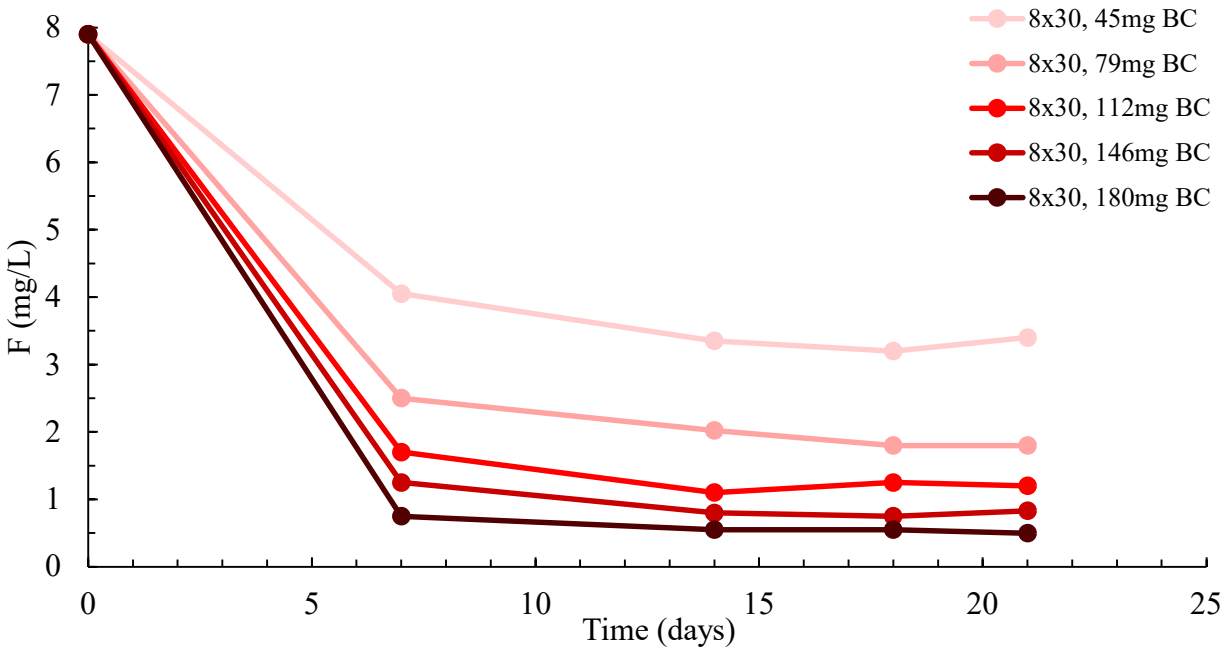

Figure S.2. Batch test data showing pseudo-equilibrium after 14-days of shaking for 8x30# size BC particles (GW^{well}).

Table S.1. Batch isotherm parameters calculated at 14-day equilibrium time with 95% CI

Size Fraction	d_p *(mm)*	K_F *((mg/g)(L/mg)$^{1/n}$)*		*1/n*	
		NC	*MX*	*NC*	*MX*
8x30#	1.29	3.00±0.17	2.73±0.21	0.38±0.06	0.49±0.09
30x60#	0.40	3.14±0.08	3.03±0.26	0.38±0.03	0.50±0.11
60x100#	0.20	3.01±0.14	3.03±0.50	0.40±0.06	0.42±0.20
100x200#	0.11	3.55±0.12	3.01±0.38	0.36±0.04	0.45±0.16

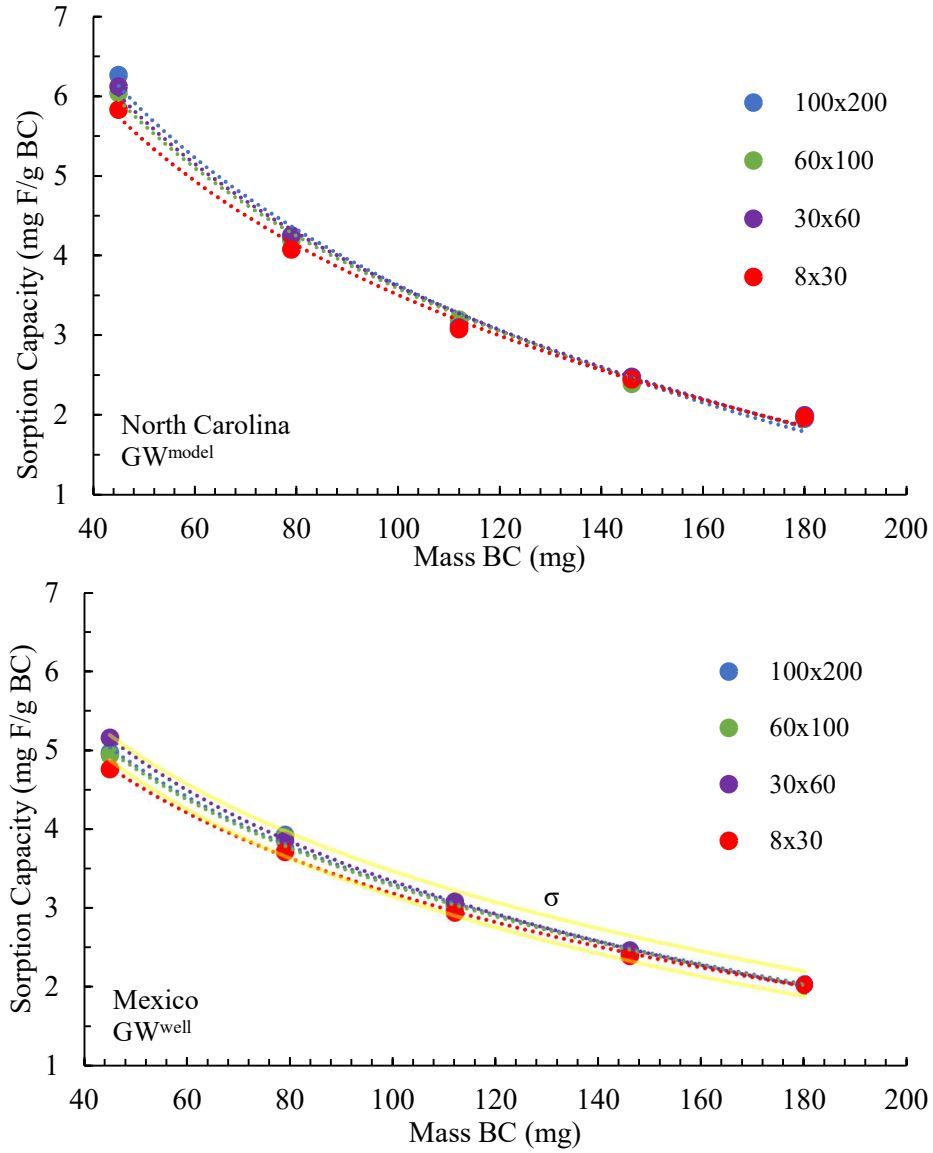

Figure S.3. Average sorption capacity of BC size fraction by mass.
Most data fall within one standard deviation (σ, yellow bounds on MX graph). This shows particle size does not increase sorption capacity. Data spread decreases with increasing BC mass which may be due to increased weighing accuracy at higher mass doses.

3.3. DCBR

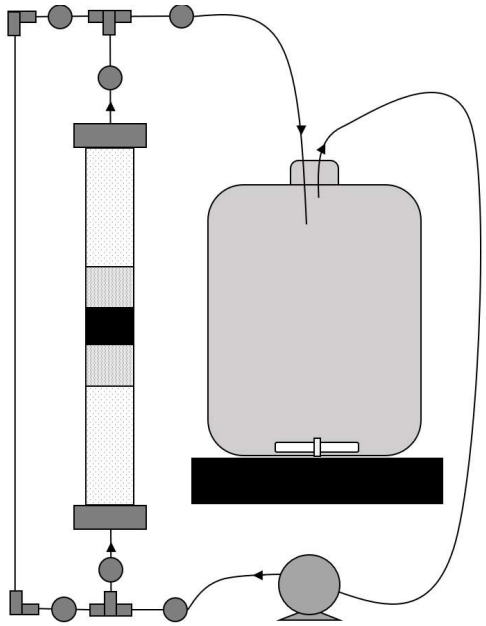

Figure S.4. DCBR apparatus diagram.
Solution passes through a packed bed of sorbent media and is recirculated into the continuously stirred tank.

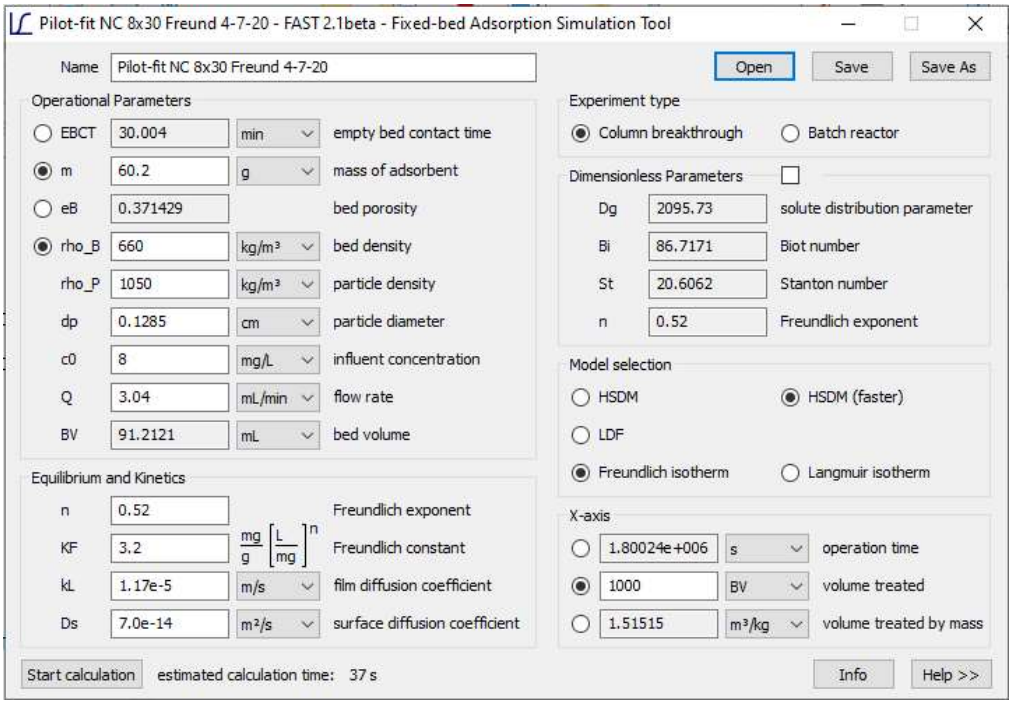

Figure S.5. FAST interface.

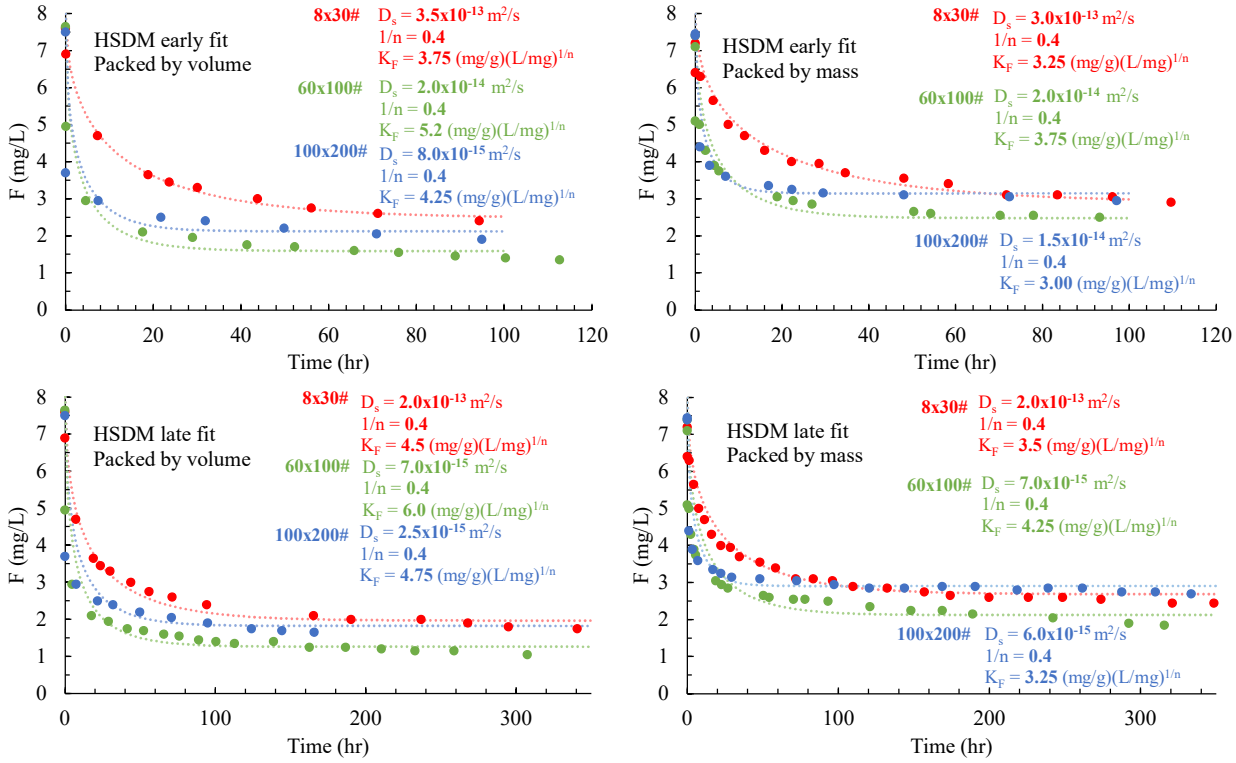

Figure S.6. DCBR data fit with the HSDM to determine equilibrium and kinetic parameters.

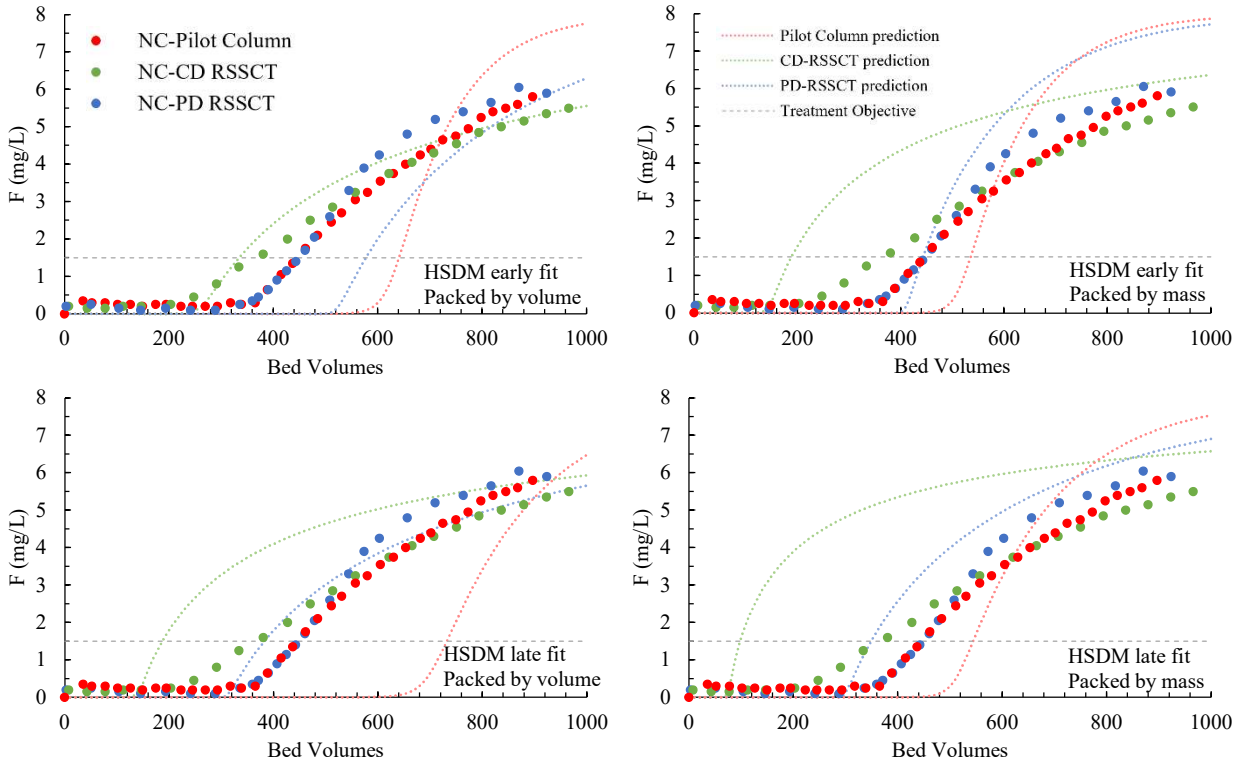

Figure S.7. Column predictions using the FAST with kinetic and equilibrium inputs from DCBR fits (see Figure S.6 for inputs)

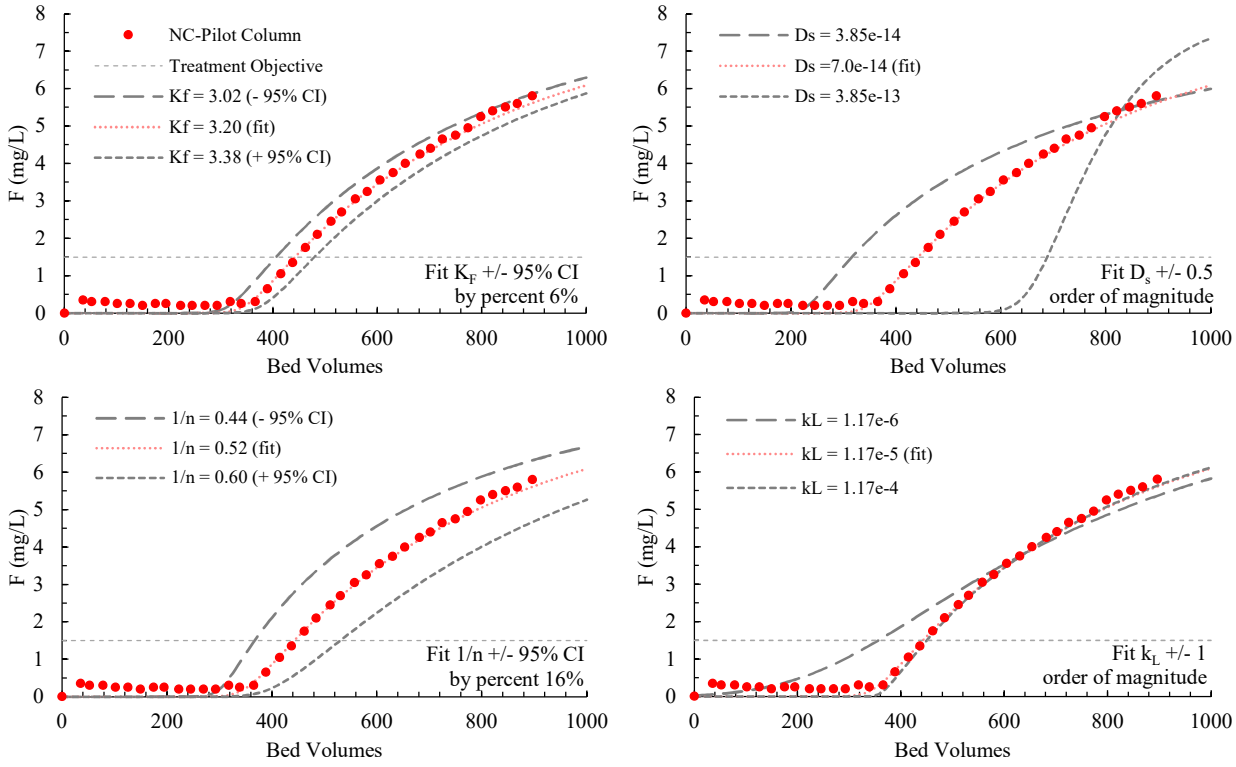

Figure S.8. HSDM sensitivity analysis of 1/n, K_F, k_L, D_s for NC-Pilot best-fit. 1/n and K_F were varying over a 95% CI calculated from batch test data. D_s and k_L were varied over a half order of magnitude and full order of magnitude around the best-fit, respectively.

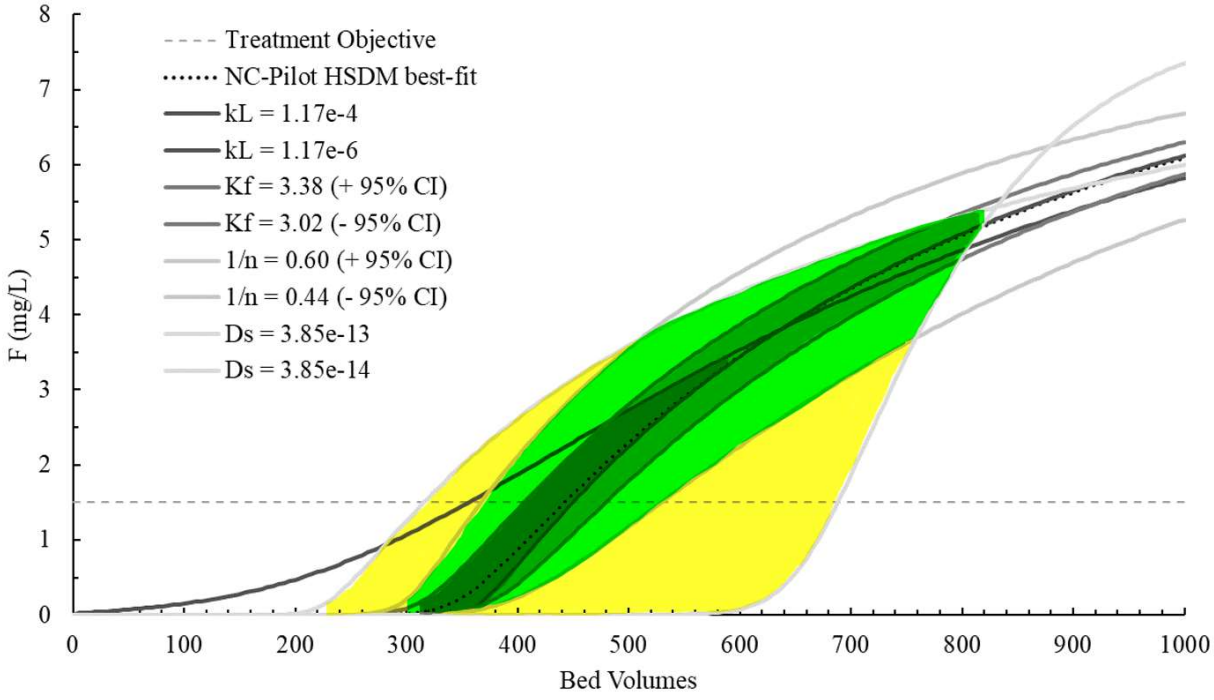

Figure S.9. Heat-map of model input (1/n, K_F, k_L, D_s) sensitivity analysis showing the regions of overlap around the NC-Pilot best-fit.

3.4. Experimental Factors

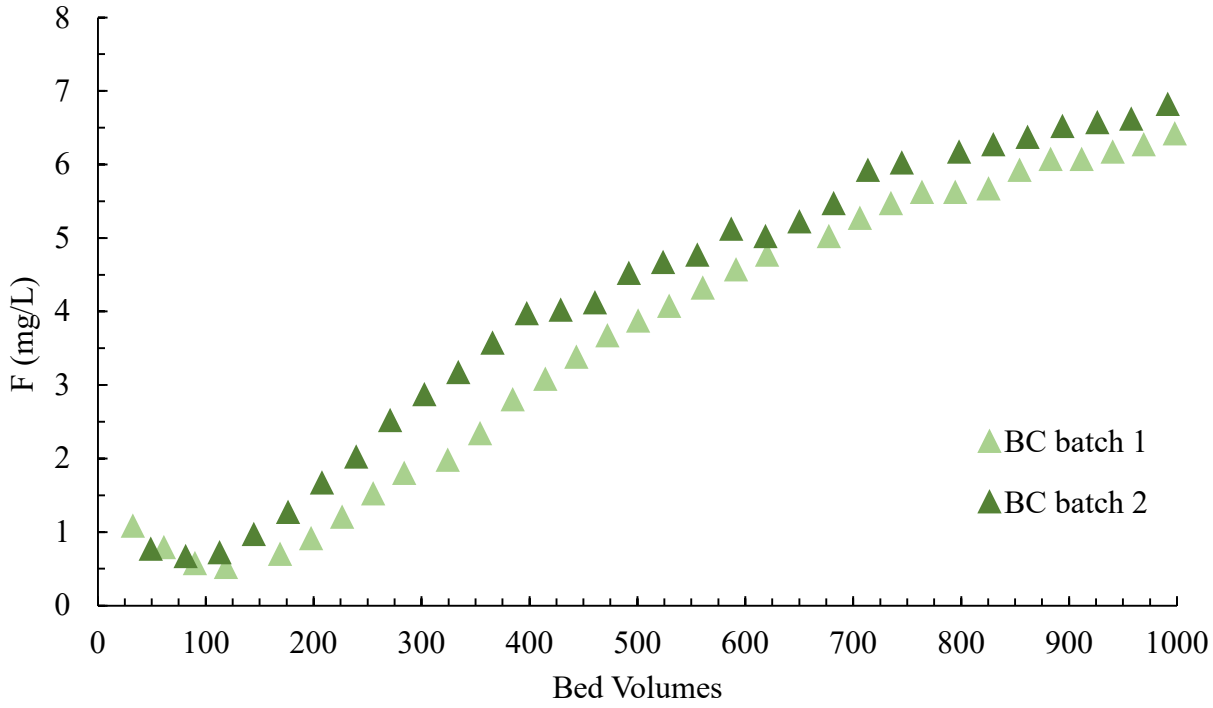

Figure S.10. Impact of BC batch on column breakthrough (CD-RSSCT, GW^{well}).

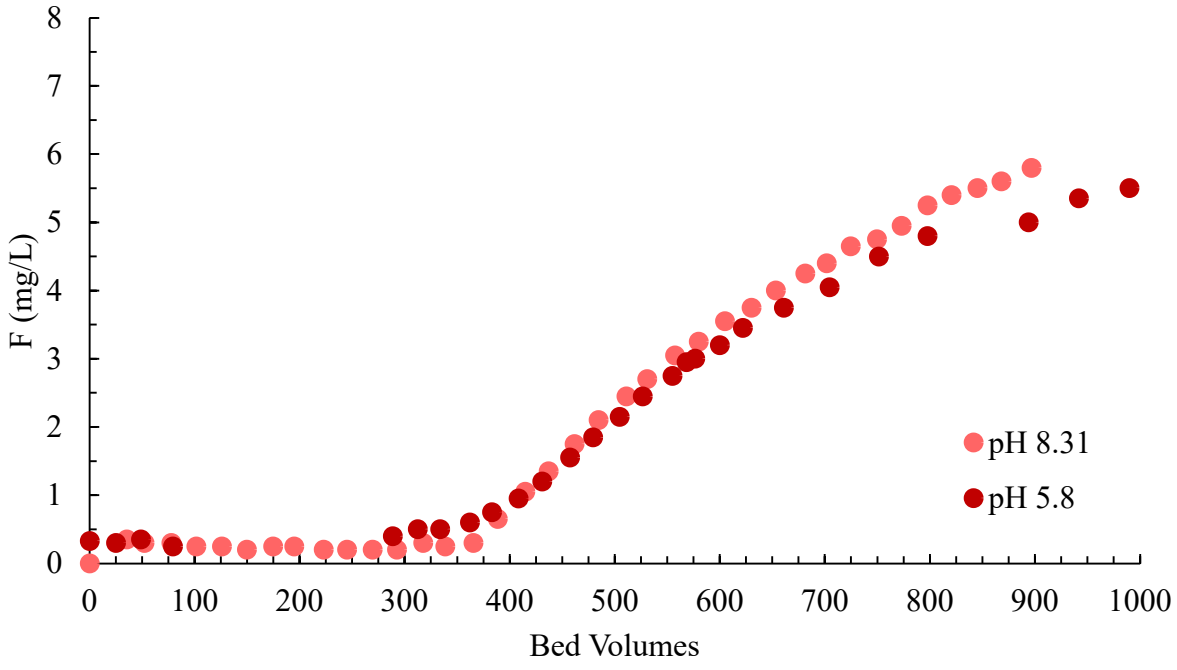

Figure S.11. Impact of solution pH on column breakthrough (Pilot Column, GW^{model}).

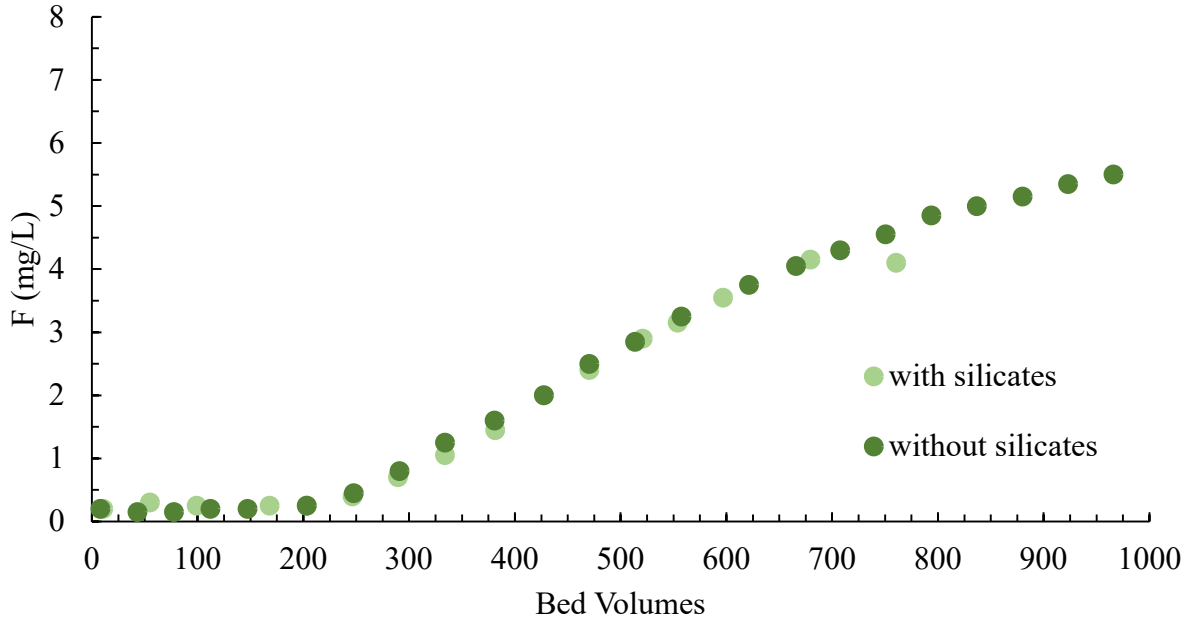

Figure S.12. Impact of silicate content on column breakthrough (CD-RSSCT, GW^{model}).

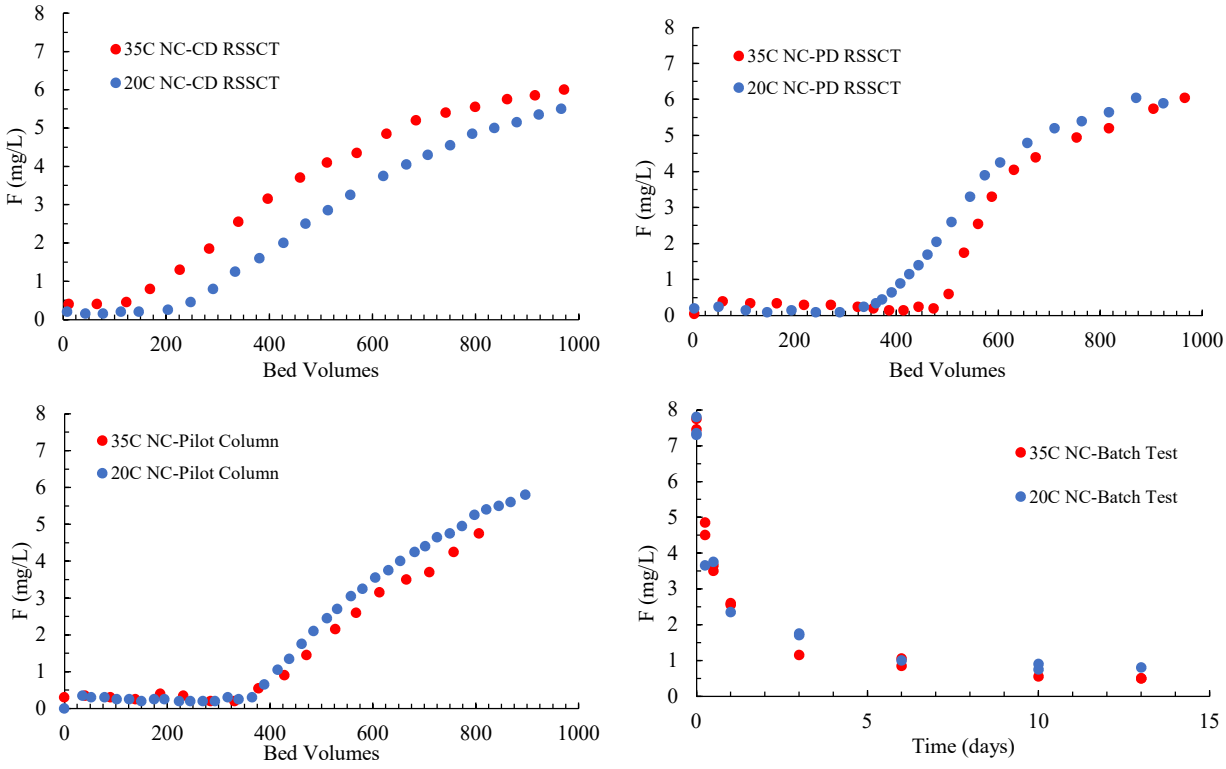

Figure S.13. Impact of temperature on F uptake in columns and batch tests (GW^{model}).

3.5. Column Design

Table S.2. Mass transfer model parameters used in RSSCT design

Parameter	*Equation*
Pore diffusion modulus (Ed)	$Ed = \frac{4LD_g D_L \varepsilon}{{d_p}^2 v_f \tau}$
Stanton number (St)	$St = \frac{2k_f L(1-\varepsilon)}{d_p v_f}$
Peclet number (Pe)	$Pe = \frac{v_f L}{\varepsilon D_L \left[0.67 + 0.5\left(\frac{d_p v_f}{\varepsilon D_L}\right)^{1.2}\right]}$
Pore solute distribution parameter (Dg)	$Dg = \frac{\varepsilon_p(1-\varepsilon)}{\varepsilon}$
Reynolds number (Re)	$Re = \frac{\rho_w v_f d_p}{\varepsilon \mu_w}$
Schmidt number (Sc)	$Sc = \frac{\mu_w}{\rho_w D_L}$
Biot number (Bi)	$Bi = \frac{k_f d_p \tau}{2D_L \varepsilon_p}$
Sherwood number (Sh)	$Sh = [1 + 1.5(1-\varepsilon)]Sh_p$
Sherwood number single particle (Sh_p)	$Sh_p = 2 + \sqrt{{Sh_{lam}}^2 + {Sh_{turb}}^2}$
Sherwood number laminar conditions (Sh_{lam})	$Sh_{lam} = 0.664 Sc^{\frac{1}{3}} Re^{\frac{1}{2}}$
Sherwood number turbulent conditions (Sh_{turb})	$Sh_{turb} = \frac{0.037 Re^{0.8} Sc}{1 + 2.443 Re^{-0.1}\left(Sc^{\frac{2}{3}} - 1\right)}$
Liquid diffusivity (D_L) ($cm^2\ sec^{-1}$)	$D_L = \frac{1.326e-4}{\left[(100\mu_w)^{1.14} {V_b}^{0.589}\right]}$
Film mass transfer coefficient (k_f) ($cm\ sec^{-1}$)	$k_f = \frac{D_L}{d_p} Sh$

Variable definitions:

L = bed depth (cm)

d_p = particle diameter (cm)

ε_p = particle porosity; ~ 0.5 (Leyva-Ramos et al., 2010)

ε = bed porosity; ~ 0.37 (Leyva-Ramos et al., 2010)

μ_w = dynamic viscosity of water (poise, 9.32×10^{-3} g cm^{-1} sec^{-1})

ρ_w = density of water (0.998 g cm^{-3})

V_b = molar volume of adsorbate (cm^3 mol^{-1})

v_f = velocity (hydraulic loading rate, HLR) (cm sec^{-1})

τ = tortuosity; ~ 3 (Leyva-Ramos et al., 2010)

ϕ = particle shape correction factor (typical value 1)

Chapter 4: For Practitioners - Techniques for Optimizing Bone-char Column Design

The desired outcome of this study was to develop a workflow for quantifying fluoride removal by bone-char sorbents from groundwater to be used in a field-lab setting by presenting practitioners with tools necessary to determine effective defluoridation materials through the use of the RSSCT and HSDM. Bone-char used in this study was produced on a community scale using waste materials collected from a local butchery, fluoride impacted groundwater was sources from a well located on rural farm, and all column and batch experiments were duplicated in a field lab to assess feasibility. This study successfully applied the RSSCT method for full-scale contactor performance prediction in a lab setting but was unable to match small-scale breakthrough to large-scale breakthrough treating natural water. This highlights the importance of conducting tests in the field using natural water of the same background chemistry to that used in community systems. The CD-RSSCT provided a conservative (~ 100 BV) estimation of full-scale contactor performance in both waters and is the recommended method for community system design based on the findings of this study.

Chapter 5: Next Steps

The next steps for this research include extending the RSSCT approach to more sorbents (chemically modified BC, granular ferric oxides, etc.) and other GW chemistries in regions impacted by elevated F. Temperature dependence of char should also be explored to determine the influence on community systems as well as comparing more full-scale systems in communities to validate the RSSCT approach. This study tested two batches of BC produced at the same production site using the same raw bone material. Studies comparing bone-type found little difference in sorption capacity, but none compared raw BC materials for SC prediction. Other inorganic contaminant systems may also benefit from SC tests such as granular ferric oxide systems for As removal. Small-columns should be operated with the same water as large-columns for accurate breakthrough prediction. Other natural GW chemistries may impact SC tests differently and may further validate the RSSCT approach. Temperature influence on BC uptake of F was not determined in this study and should be tested further.

REFERENCES

Abaire, B., Zewge, F., & Endalew, M. (2009). Operational experiences on small-scale community defluoridation systems. In *Water, sanitation and hygiene: sustainable development and multisectoral approaches.* 34th Water, Engineering and Development Centre International Conference, Addis Ababa, Ethiopia.

Abe, I., Iwasaki, S., Tokimoto, T., Kawasaki, N., Nakamura, T., & Tanada, S. (2004). Adsorption of fluoride ions onto carbonaceous materials. *Journal of Colloid Interface Science, 275*(1), 35-39.

Amini, M., Mueller, K., Abbaspour, K. C., Rosenberg, T., Afyuni, M., Moller, K. N., . . . Johnson, C. A. (2008). Statistical Modeling of Global Geogenic Fluoride Contamination in Groundwaters. *Environmental Science & Technology, 42*(10), 3662-3668.

Ayoob, S., Gupta, A. K., & Bhat, V. T. (2008). A Conceptual Overview on Sustainable Technologies for the Defluoridation of Drinking Water. *Critical Reviews in Environmental Science and Technology, 38*(6), 401-470.

Badruzzaman, M., Westerhoff, P., & Knappe, D. R. (2004). Intraparticle diffusion and adsorption of arsenate onto granular ferric hydroxide (GFH). *Water Research, 38*(18), 4002-4012.

Bolster, C. H. (2010). Microsoft Excel Spreadsheets for Fitting Sorption Data. Bowling Green, KY: United States Department of Agriculture. Agricultural Research Service (USDA-ARS).

Brunson, L. R., & Sabatini, D. A. (2009). An Evaluation of Fish Bone Char as an Appropriate Arsenic and Fluoride Removal Technology for Emerging Regions. *Environmental Engineering Science, 26*.

Brunson, L. R., & Sabatini, D. A. (2014). Practical considerations, column studies and natural organic material competition for fluoride removal with bone char and aluminum amended materials in the Main Ethiopian Rift Valley. *Science of the Total Environment, 488*, 584-591.

Caminos de Agua. (2019). *Fluoride Levels in Rural Guanajuato Community Well Water. Water Quality Monitoring Web Database.* Retrieved from caminosdeagua.org/en/water-quality-monitoring

Chatterjee, S., Jha, S., & De, S. (2018). Novel carbonized bone meal for defluoridation of groundwater: Batch and column study. *Journal of environmental science and health. Part A, Toxic/hazardous substances & environmental engineering, 53*(9), 832-846.

Chatterjee, S., Mukherjee, M., & De, S. (2018). Defluoridation using novel chemically treated carbonized bone meal: batch and dynamic performance with scale-up studies. *Environmental Science & Pollution Research, 25*(18), 18161-18178.

Cheung, C.-W., Choy, K. K. H., Porter, J. F., & McKay, G. (2005). Empirical Multicomponent Equilibrium and Film-Pore Model for the Sorption of Copper, Cadmium and Zinc onto Bone Char. *Adsorption, 11*(1), 15-29.

Crittenden, J. C., Berrigan, J. K., & Hand, D. W. (1986). Design of Rapid Small-Scale Adsorption Tests for a Constant Diffusivity. *Journal (Water Pollution Control Federation), 58*, 312-319.

Crittenden, J. C., Berrigan, J. K., Hand, D. W., & Lykins, B. (1987). Design of Rapid Fixed-Bed Adsorption Tests for Nonconstant Diffusivities. *Journal of Environmental Engineering, 113*.

Díaz-Barriga, F., Leyva, R., Quistían, J., Loyola-Rodríguez, J. P., Pozos, A., & Grimaldo, M. (1997). Endemic fluorosis in San Luis Potosi, Mexico. IV Source of fluoride exposure. *Fluoride, 30*(4), 219-222.

Díaz-Barriga, F., Navarro-Quezada, A., Grijalva, M. I., Grimaldo, M., Loyola-Rodriguez, J. P., & Ortz, M. D. (1997). Endemic fluorosis in Mexico. *Fluoride, 30*(4), 233-239.

Fawell, J., Bailey, K., Chilton, J., Dahi, E., Fewtrell, L., & Magara, Y. (2006). Fluoride in Drinking-water. *World Health Organization (WHO)*.

Hand, D. W., Crittenden, J. C., & Thacker, W. E. (1983). User-Oriented Batch Reactor Solutions to the Homogeneous Surface-Diffusion Model. *Journal of Environmental Engineering, 109*(1), 82-101.

Irigoyen-Camacho, M. E., García Pérez, A., Mejía González, A., & Huizar Alvarez, R. (2016). Nutritional status and dental fluorosis among schoolchildren in communities with different drinking water fluoride concentrations in a central region in Mexico. *Science of the Total Environment, 541*, 512-519.

Kawasaki, N., Ogata, F., Tominaga, H., & Yamaguchi, I. (2009). Removal of fluoride ion by bone char produced from animal biomass. *Journal of Oleo Science, 58*(10), 529-535.

Kearns, J., Krupp, A., Diek, E., Mitchell, S., Dossi, S., & Hartman, S. (2018). Lead-lag series and staged parallel operational strategies improve the performance and cost-effectiveness of bonechar for control of fluoride in groundwater. *Journal of Water, Sanitation and Hygiene for Development, 8*(4), 777-784.

Kennedy, A. M., & Arias-Paic, M. (2020). Fixed-Bed Adsorption Comparisons of Bone Char and Activated Alumina for the Removal of Fluoride from Drinking Water. *Journal of Environmental Engineering, 146*(1).

Knappett, P. S. K., Li, Y., Hernandez, H., Rodriguez, R., Aviles, M., Deng, C., . . . Datta, S. (2018). Changing recharge pathways within an intensively pumped aquifer with high fluoride concentrations in Central Mexico. *Science of the Total Environment, 622-623*, 1029-1045.

Leyva-Ramos, R., Rivera-Utrilla, J., Medellin-Castillo, N. A., & Sanchez-Polo, M. (2010). Kinetic modeling of fluoride adsorption from aqueous solution onto bone char. *Chemical Engineering Journal, 158*(3), 458-467.

Medellin-Castillo, N. A., Leyva-Ramos, R., Ocampo-Perez, R., de la Cruz, R. F. G., Aragon-Pina, A., Martinez-Rosales, J. M., . . . Fuentes-Rubio, L. (2007). Adsorption of fluoride from water solution on bone char. *Industrial & Engineering Chemistry Research, 46*(26), 9205-9212.

Medellin-Castillo, N. A., Leyva-Ramos, R., Padilla-Ortega, E., Ocampo-Perez, R., Flores-Cano, J. V., & Berber-Mendoza, M. S. (2014). Adsorption capacity of bone char for removing fluoride from water solution. Role of hydroxyapatite content, adsorption mechanism and competing anions. *Journal of Industrial and Engineering Chemistry, 20*(6), 4014-4021.

Medellin-Castillo, N. A., Padilla-Ortega, E., Tovar-Garcia, L. D., Leyva-Ramos, R., Ocampo-Perez, R., Carrasco-Marin, F., & Berber-Mendoza, M. S. (2016). Removal of fluoride from aqueous solution using acid and thermally treated bone char. *Adsorption, 22*(7), 951-961.

Mjengera, H., & Mkongo, G. (2003). Appropriate deflouridation technology for use in flourotic areas in Tanzania. *Physics and Chemistry of the Earth, 28*(20-27), 1097-1104.

Murray, J. J. (1986). *Appropriate Use of Fluorides for Human Health*: World Health Organization. Geneva.

Nigri, E. M., Cechinel, M. A. P., Mayer, D. A., Mazur, L. P., Loureiro, J. M., Rocha, S. D. F., & Vilar, V. J. P. (2017). Cow bones char as a green sorbent for fluorides removal from aqueous solutions: batch and fixed-bed studies. *ENVIRONMENTAL SCIENCE AND POLLUTION RESEARCH, 24*(3), 2364-2380.

Rojas-Mayorga, C. K., Bonilla-Petriciolet, A., Aguayo-Villarreal, I. A., Hernandez-Montoya, V., Moreno-Virgen, M. R., Tovar-Gomez, R., & Montes-Moran, M. A. (2013). Optimization of pyrolysis conditions and adsorption properties of bone char for fluoride removal from water. *Journal of Analytical and Applied Pyrolysis, 104*, 10-18.

Rojas-Mayorga, C. K., Bonilla-Petriciolet, A., Sanchez-Ruiz, F. J., Moreno-Perez, J., Reynel-Avila, H. E., Aguayo-Villarreal, I. A., & Mendoza-Castillo, D. I. (2015). Breakthrough curve modeling of liquid-phase adsorption of fluoride ions on aluminum-doped bone char using micro-columns: Effectiveness of data fitting approaches. *Journal of Molecular Liquids, 208*, 114-121.

Schimmelpfennig, S., & Sperlich, A. (2011). Fixed-bed Adsorption Simulation Tool (FAST) (Version 2.1). Retrieved from http://www.fast-software.de/

Sorlini, S., Palazzini, D., & Collivignarelli, C. (2011). Fluoride removal from drinking water in Senegal: laboratory and pilot experimentation on bone char-based treatment. *Journal of Water, Sanitation and Hygiene for Development, 1*(4), 213-223.

Westerhoff, P., Highfield, D., Badruzzaman, M., & Yoon, Y. (2005). Rapid Small-Scale Column Tests for Arsenate Removal in Iron Oxide Packed Bed Columns. *Journal of Environmental Engineering, 131*(2), 262-271.

WHO. (2017). *Guidelines for Drinking-water Quality: fourth edition incorporating the first addendum.* (4th ed.). Geneva, Switzerland.

Yami, T. L., Butler, E. C., & Sabatini, D. A. (2016). Chemically activated cow bone for increased fluoride removal from drinking water. *Journal of Water Sanitation and Hygiene for Development, 6*(2), 215-223.

Yami, T. L., Chamberlain, J. F., Butler, E. C., & Sabatini, D. A. (2017). Using a High-Capacity Chemically Activated Cow Bone to Remove Fluoride: Field-Scale Column Tests and Laboratory Regeneration Studies. *Journal of Environmental Engineering, 143*(2).

Yami, T. L., Du, J. Y., Brunson, L. R., Chamberlain, J. F., Sabatini, D. A., & Butler, E. C. (2015). Life cycle assessment of adsorbents for fluoride removal from drinking water in East Africa. *International Journal of Life Cycle Assessment, 20*(9), 1277-1286.